

The Formation of the First Stars in the Universe

Simon Glover

*Department of Astrophysics, American Museum of Natural History,
Central Park West at 79th Street, New York, NY 10024*

Abstract. In this review, I survey our current understanding of how the very first stars in the universe formed, with a focus on three main areas of interest: the formation of the first protogalaxies and the cooling of gas within them, the nature and extent of fragmentation within the cool gas, and the physics – in particular the interplay between protostellar accretion and protostellar feedback – that serves to determine the final stellar mass.

In each of these areas, I have attempted to show how our thinking has developed over recent years, aided in large part by the increasing ease with which we can now perform detailed numerical simulations of primordial star formation. I have also tried to indicate the areas where our understanding remains incomplete, and to identify some of the most important unsolved problems.

Keywords: stars: formation — galaxies: formation — cosmology: theory

1. Introduction

For more than a decade – ever since the first release of the COBE results (Mather *et al.*, 1990; Smoot *et al.*, 1992) – astrophysicists and cosmologists have found themselves in the unusual situation of knowing more about the state of the universe when it was only 380,000 years old than when it was 200 million years old. Increasingly precise measurements of the cosmic microwave background (CMB), as exemplified by the recent results from WMAP (Bennett *et al.*, 2003), together with a broad range of other observational constraints (Riess *et al.*, 1998; Perlmutter *et al.*, 1999; Bahcall *et al.*, 1999; Valentine, Saunders, and Taylor, 2000; Freedman *et al.*, 2001; Percival *et al.*, 2001; O’Meara *et al.*, 2001; Kirkman *et al.*, 2003) have helped to confirm that we live in a flat universe, with approximately 5% of the closure density being provided by baryons, 25% by cold dark matter (CDM), and the remaining 70% by some form of ‘dark energy’ or cosmological constant. Models of such a universe – generally known as Λ CDM models – have been heavily studied for a number of years (see, e.g. Sugimoto and Suto, 1991; Carroll, Press, and Turner, 1992; Gnedin, 1996ab) and many of their features are well understood. For instance, the evolution of the small inhomogeneities in the early universe that give rise to the observed temperature anisotropies in the CMB can be followed in great detail



© 2018 Kluwer Academic Publishers. Printed in the Netherlands.

(Seljak and Zaldarriaga, 1996), and the resulting predictions have been strongly confirmed by the WMAP results.

The evolution of the dark matter component of the universe subsequent to the epoch of last scattering at $z \simeq 1100$ has also been studied intensively, using a wide range of techniques (see, for instance Seljak, 2000; Benson *et al.*, 2001; Cooray and Sheth, 2002). The general agreement between the results of these studies and an increasing number of observational tests (e.g. Gray *et al.*, 2002) has lent further support to this overall picture, although some puzzles remain (Moore *et al.*, 1999; Navarro and Steinmetz, 2000).

When it comes to understanding the behaviour of the baryonic component, however, we are on much shakier ground. Although cosmological perturbation theory has given us a fairly good understanding of the behaviour of the baryons in the linear regime (Gnedin and Hui, 1998; Meiksin, White, and Peacock, 1999; Singh and Ma, 2002), many details of the non-linear evolution of the baryons and the development of stars and galaxies are not understood. At the same time, we have little or no observational data to guide us. Although we now have observational probes of the Universe at redshifts $z > 6$, thanks to the success of the Sloan Digital Sky Survey at finding high-redshift quasars (Fan *et al.*, 2003), the strong metal lines observed in many of these quasars (Fan *et al.*, 2001) are evidence that we are not yet probing the earliest epochs of star formation.

Since observational limitations prevent us, for the time being, from directly studying the formation of the first stars and galaxies, work in this area has been primarily theoretical in nature. Although developing a theoretical understanding of primordial star formation may seem at first to be a hopelessly optimistic ambition – after all, there is still much that we do not understand about local star formation, despite the large quantity of observational data available to us – there are actually several good reasons to think that the problem may be a simpler one than understanding present day star formation.

First, the initial conditions – small perturbations to a uniform cosmological background – are simple and well understood (provided that the Λ CDM model remains as accurate on small scales as it has proved to be on the larger scales probed by galaxy surveys and the CMB). Second, the chemistry of primordial gas is also simple, at least in comparison to that of present day molecular clouds. It is therefore much easier to identify the critical reactions and to numerically simulate the chemical evolution of the gas. Third, magnetic fields, if present, are unlikely to be dynamically significant (Widrow, 2002); consequently, they are usually ignored. Finally, by restricting our attention to the first generation of stars to form, we can avoid the many complications posed by the

feedback of stars on their surroundings (see, for instance, Glover, 2001 and references therein).

Nevertheless, the problem remains a challenging one that involves processes occurring over a very wide range of length scales, from the cosmological to the protostellar. A popular approach is to break this problem up into a series of simpler problems, with different characteristic scales, that can be tackled individually. For instance:

- (i) When do the first protogalaxies¹ form, and how massive are they?
- (ii) How does gas evolve within these protogalaxies? Does it fragment, and if so, how large are the resulting fragments? When and why does fragmentation stop?
- (iii) What is the initial mass function (IMF) of the first stars, and what processes determine this?

In this article, I review our progress at answering these questions. The body of the review is divided into three sections, each with a theme that broadly reflects one of the questions posed above, although there is inevitably a certain amount of overlap.

There are, of course, many interesting questions concerning the first stars and galaxies which I have neither the time nor the space to properly address in this review; for instance, the question of how best to go about observing them; or the question of how they affect their environment both on small and large scales. Some of these questions are addressed in other recent reviews of early star formation (Barkana and Loeb, 2001; Bromm and Larson, 2004; Ciardi and Ferrara, 2004), which complement the material presented here.

Throughout this paper, unless otherwise indicated, I adopt cosmological parameters taken from the WMAP concordance model (Spergel *et al.*, 2003). Specifically: $\Omega_m = 0.29$, $\Omega_\Lambda = 0.71$, $\Omega_b = 0.047$, $h = 0.72$, $\sigma_8 = 0.9$, $n_s = 0.99$.

2. The formation of protogalaxies

2.1. THE FIRST BOUND OBJECTS

In CDM models, gravitationally bound objects form in a hierarchical, or ‘bottom-up’ fashion, with the smallest, least massive objects forming

¹ A note on terminology: in this review, I use the term ‘protogalaxy’ as a convenient shorthand for ‘gravitationally bound gas cloud’: the fact that something is described as a protogalaxy does not imply that it is actively forming stars, merely that it has the potential to do so.

first, and larger objects forming later through a mixture of mergers and accretion. The mass scale on which gravitationally bound objects begin to form (i.e. the minimum mass of a bound object) is set by the free streaming of the dark matter particles (Blumenthal *et al.*, 1984). In general, this mass scale is many orders of magnitude smaller than scales of cosmological interest; for instance, in the neutralino model for CDM, $M_{\min} \simeq 10^{-7} M_{\odot}$ (Hofmann, Schwarz, and Stöcker, 2001). However, the subsequent formation of larger objects occurs rapidly, and at most redshifts a large number of gravitationally bound objects (frequently referred to as ‘dark matter halos’) exist, with a wide range of different masses.

Considerable effort has been devoted to determining the mass function of dark matter halos as a function of redshift. The most widely used expression for the mass function is one originally suggested by Press and Schechter (1974):

$$n(M, z) dM = \sqrt{\frac{2}{\pi}} \frac{\rho_{\text{dm}}}{M} \frac{d\nu}{dM} \exp\left(-\frac{\nu^2}{2}\right) dM. \quad (1)$$

Here $n(M, z) dM$ is the comoving number density of halos at redshift z with dark matter masses in the interval $(M, M + dM)$, ρ_{dm} is the cosmological background density of dark matter, and $\nu \equiv \delta_c/[D(z)\sigma(M)]$, where δ_c is a critical overdensity (generally taken to be 1.69), $D(z)$ is the linear growth factor (Peebles, 1980; Carroll, Press, and Turner, 1992) and $\sigma(M)$ is the rms fluctuation in the cosmological density field of dark matter smoothed on a mass scale M . A comprehensive discussion of the derivation of this equation is given in Bond *et al.* (1991).

Comparisons with the results of N-body simulations at low redshift (Jenkins *et al.*, 2001) and at high redshift (Jang-Condell and Hernquist, 2001) demonstrate that the Press-Schechter mass function provides a reasonable fit to the true mass function, although a better fit to the simulation results can be obtained by using a modified form suggested by Sheth and Tormen (1999):

$$n(M, z) dM = A \left(1 + \frac{1}{\nu'^{2q}}\right) \sqrt{\frac{2}{\pi}} \frac{\rho_{\text{dm}}}{M} \frac{d\nu'}{dM} \exp\left(-\frac{\nu'^2}{2}\right) dM, \quad (2)$$

where $\nu' = \sqrt{a}\nu$, $a = 0.707$, $A \simeq 0.322$ and $q = 0.3$.

In either case, the basic form of the mass function is the same: it behaves as a power law for $\nu \ll 1$ and falls off exponentially for $\nu \gg 1$. In CDM models, $\sigma(M)$ decreases monotonically with increasing mass, and so the most massive objects will also be the rarest. The transition to exponential behaviour occurs for $\nu \sim 1$, or $\sigma(M) \sim \delta_c/D(z)$, and

so this transition occurs at a progressively smaller mass as we move to higher redshifts.

Given a mass function of this type, is there any way to specify when the first halo of a given mass forms? Strictly speaking, the answer is no; the probability of finding a halo of any finite mass is never zero. In practice, however, we are more interested in determining when this probability grows to some interesting size, or when the number density of halos exceeds some specified threshold (which amounts to the same thing). This is most commonly done by specifying a value of ν which is of interest; for instance, reference is often made to 3σ halos, which are simply halos for which $\nu = 3$ and which therefore have a dark matter mass M satisfying:

$$\sigma(M) = \frac{1}{3} \frac{\delta_c}{D(z)}. \quad (3)$$

Such halos are moderately rare objects, representing no more than a few thousandths of the total cosmic mass (Mo and White, 2002), but are sufficiently common that one would expect to find many of them within a single Hubble volume. They are often taken to be representative of the earliest objects to form, although this choice is somewhat arbitrary.

Unfortunately, while the Press-Schechter approach allows us to determine when the first dark matter halos of a given mass form, it does not, by itself, tell us when the first *protogalaxies* form, as it contains no information about the behaviour of the baryonic component of the universe. Unlike the dark matter, the baryons do not initially form structures on very small scales, since pressure forces act to suppress the growth of small-scale perturbations (Jeans, 1902; Jeans, 1928; Bonnor, 1957). We can estimate the scale on which pressure forces become significant by equating the sound-crossing timescale, t_{sc} , with the gravitational free-fall timescale, t_{ff} : if $t_{\text{sc}} < t_{\text{ff}}$ then perturbations can respond subsonically to changes in the gravitational field and will therefore remain in approximate hydrostatic equilibrium; on the other hand, if $t_{\text{sc}} > t_{\text{ff}}$ then perturbations cannot respond subsonically, and some degree of gravitational collapse becomes inevitable. In gas with a density ρ and sound speed c_s , we would therefore expect collapse to be suppressed on scales

$$\lambda \lesssim \frac{c_s}{\sqrt{G\rho}}. \quad (4)$$

A more careful analysis using linear perturbation theory (Peebles, 1980) shows that in a purely baryonic universe, the growth of perturbations is completely suppressed on scales smaller than

$$\lambda_{\text{J}} \leq \frac{\pi^{1/2} c_s}{\sqrt{G\rho_{\text{b}}}}, \quad (5)$$

where ρ_b is the cosmological baryon density. This critical wavelength is commonly known as the Jeans length. The associated mass scale, known as the Jeans mass, is conventionally defined as

$$M_J = \frac{4}{3}\pi\rho_b \left(\frac{\lambda_J}{2}\right)^3. \quad (6)$$

The value of the Jeans mass depends on the baryon density, which is a simple function of redshift, and on the temperature of the intergalactic medium (through the dependence of λ_J on c_s). The latter is simple to calculate at epochs prior to the onset of widespread star formation and is well approximated by (Galli and Palla, 1998)

$$T = 410 \left(\frac{1+z}{150}\right)^2 \text{ K} \quad (7)$$

for redshifts $z < 150$. The corresponding Jeans mass at these redshifts is given by

$$M_J = \frac{4.9 \times 10^4}{(\Omega_b h^2)^{1/2}} \left(\frac{1+z}{150}\right)^{3/2} M_\odot. \quad (8)$$

To generalize this to the case of a universe containing both baryons and cold dark matter, it is tempting to simply replace the baryon density in the above equations with the total density $\rho_m = \rho_b + \rho_{\text{dm}}$, which would give us

$$M_J = \frac{4.9 \times 10^4}{(\Omega_m h^2)^{1/2}} \left(\frac{1+z}{150}\right)^{3/2} M_\odot \quad (9)$$

for $z < 150$; or in other words, a Jeans mass that is a factor $(\Omega_b/\Omega_m)^{1/2}$ smaller. In fact, the situation is not so simple, as perturbations can continue to grow on small scales in the dark matter even when suppressed in the baryons. A linear treatment of this case is given in Gnedin and Hui (1998), but ultimately this treatment breaks down as small-scale structure in the dark matter begins to grow non-linearly. Although these non-linear effects have received little direct study, there is some evidence from numerical simulations that they can cause baryons to collapse on scales smaller than λ_J (see, for instance, the discussion in section 2.1 of Haiman and Loeb, 1997), although any such collapse will be significantly delayed relative to the dark matter due to the influence of the gas pressure. In view of this, it is probably best to treat the value of M_J given by Equation (9) as an estimate of the scale on which pressure effects begin to dominate, rather than as an absolute lower limit to the protogalactic mass.

Given M_J , we can go on to estimate the mass and formation redshift of the first protogalaxies by asking when the total mass of a 3σ halo

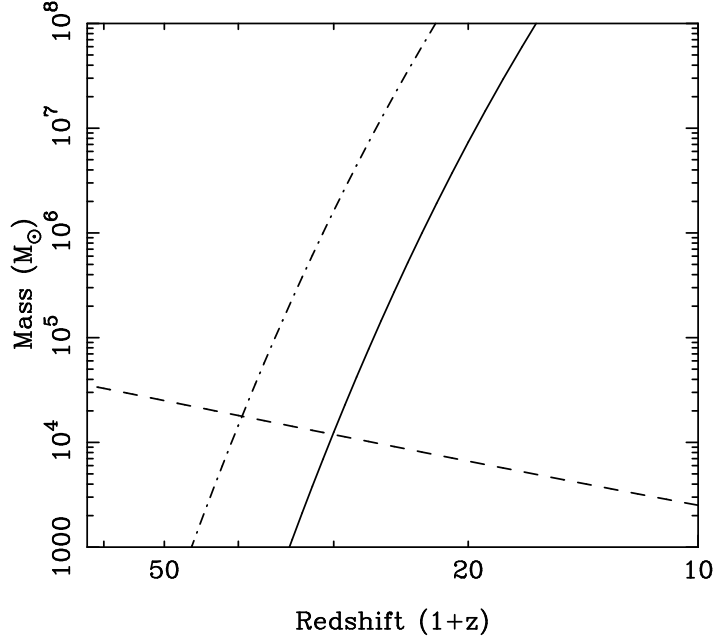


Figure 1. The evolution with redshift of $M_{3\sigma}$ (solid line), $M_{4\sigma}$ (dot-dashed line) and M_J (dashed line). Protogalaxies will develop within 3σ dark matter halos once the mass of dark matter in the halo, $M_{3\sigma}$, exceeds M_J ; this occurs at $z \lesssim 30$. Similarly, protogalaxies will form in 4σ halos once their dark matter mass, $M_{4\sigma}$, exceeds M_J , which occurs at $z \lesssim 40$.

first exceeds the Jeans mass. To properly answer this question, we would need to know the baryon fraction of these protogalaxies (i.e. their ratio of baryonic to dark matter). In practice, however, we know that this will be small and that the protogalactic mass will be dominated by the dark matter component. Therefore, for the purposes of a simple estimate it is sufficient to compare the Jeans mass with the dark matter mass of the 3σ halo (hereafter $M_{3\sigma}$), which we can calculate using Equation (3). The evolution with redshift of both mass scales is plotted in figure 1. We can see from the figure that the first protogalaxies will have a total mass $M \sim 10^4 M_\odot$ and will form at a redshift $z \sim 30$. It is also clear that uncertainties in M_J will have little effect on the estimated redshift, due to the sharp rise in $M_{3\sigma}$ with declining z . On the other hand, the use of a different criterion to identify our ‘first’ objects (e.g. considering 4σ halos instead of 3σ ones) has a rather larger effect on z , but has very little effect on the estimated protogalactic mass.

2.2. THE IMPORTANCE OF COOLING

Once a protogalaxy has formed, the next task is to determine how the gas within it evolves. In particular, we would like to know whether *every* protogalaxy that forms is capable of forming stars, or whether there are other prerequisites.

We can gain considerable insight into this question by considering the thermal evolution of a parcel of gas that is undergoing gravitational collapse. The gravitational potential energy of the gas is transformed first into kinetic energy and thence into thermal energy through adiabatic compression, as well as the action of shocks if the flow is supersonic. Unless the gas can dissipate this thermal energy through radiative cooling, it must inevitably heat up. Since both density and temperature are rising, the pressure will increase rapidly, and ultimately will become large enough to halt the collapse.

We can make this argument more quantitative by considering the gravitational stability of small perturbations within the collapsing gas. As in the cosmological case, we can derive a minimum unstable mass scale, again termed the Jeans mass, which scales as

$$M_J \propto \frac{c_s^3}{\rho^{1/2}} \propto \frac{T^{3/2}}{\rho^{1/2}}. \quad (10)$$

If we define an effective adiabatic index

$$\gamma_{\text{eff}} = 1 + \frac{d \ln T}{d \ln \rho}, \quad (11)$$

then M_J will evolve with density as

$$M_J \propto \rho^{\frac{3}{2}(\gamma_{\text{eff}} - \frac{4}{3})}. \quad (12)$$

Therefore, if $\gamma_{\text{eff}} > 4/3$, the Jeans mass will increase during the collapse and will eventually become comparable to the mass of the protogalaxy, at which point collapse must halt. Since $\gamma_{\text{eff}} = 5/3$ for an atomic gas evolving adiabatically, it is clear that in the absence of radiative cooling, the increasing thermal pressure will bring collapse to an end long before protostellar densities are reached. Therefore, star formation is only possible if the gas can cool.

The timescale on which cooling occurs is also of great importance. It has long been argued (Gott and Thuan, 1976; Rees and Ostriker, 1977; Silk, 1977a) that the behaviour of gas in a collapsing protogalaxy depends upon the relative sizes of its cooling timescale,

$$t_{\text{cool}} = \frac{1}{\gamma - 1} \frac{nkT}{\Lambda(T)}, \quad (13)$$

(where n is the particle number density and $\Lambda(T)$ is the cooling rate per unit volume), its dynamical (or free-fall) timescale, given by

$$t_{\text{dyn}} = \sqrt{\frac{3}{32\pi G\rho}}, \quad (14)$$

and the cosmological timescale, or Hubble time,

$$t_{\text{H}} \simeq \frac{1}{H(z)}. \quad (15)$$

It is easy to show that t_{dyn} is always less than t_{H} , so there are only three possible arrangements:

- (i) $t_{\text{cool}} > t_{\text{H}} > t_{\text{dyn}}$,
- (ii) $t_{\text{H}} > t_{\text{cool}} > t_{\text{dyn}}$,
- (iii) $t_{\text{H}} > t_{\text{dyn}} > t_{\text{cool}}$.

In case (i), cooling takes place on a cosmological timescale, and is so slow that the gas evolves much as if there were no cooling at all. It quickly becomes pressure supported and remains so almost indefinitely, unless disturbed by an external event, such as a merger with another protogalaxy. In case (ii), the gas also becomes pressure supported, but subsequently contracts quasi-statically on a cosmologically interesting timescale. Finally, gas described by case (iii) never becomes pressure supported, but instead simply collapses at or near the free-fall rate.

In practice, the situation is often far more complex than this analysis suggests, since the appropriate description for gas in a given protogalaxy may vary with its location within the protogalaxy, and may also change over time as the density, temperature and/or chemical makeup of the gas change. Nevertheless, this scheme is a useful first approximation, and serves to further highlight the central role played by radiative cooling.

2.3. COOLING AND CHEMISTRY WITHIN PRIMORDIAL GAS

A number of potential cooling mechanisms exist within primordial gas (Anninos *et al.*, 1997), but many, such as Lyman- α cooling, operate only for $T > 10^4$ K, while the first protogalaxies have characteristic temperatures $T \sim 100$ – 1000 K. At these low temperatures, the dominant coolant is molecular hydrogen, H_2 , the most abundant primordial molecule. Therefore, to determine the cooling rate accurately, we require an accurate value for the H_2 abundance, which means that in

addition to studying the thermal evolution of the gas we must also study its chemical evolution.

The chemistry of primordial gas has been investigated by a number of authors (Dalgarno and Lepp, 1987; Black, 1991; Abel *et al.*, 1997; Galli and Palla, 1998; Stancil, Lepp, and Dalgarno, 1998, 2002) and proves to be surprisingly complex despite the limited number of elements involved. This complexity is due to the wide variety of different molecules and molecular ions that can be formed. However, if we are only interested in those aspects of the chemistry that affect the cooling rate, then we can make substantial simplifications (Abel *et al.*, 1997): the chemical model can be reduced to a few processes that determine the ionization balance of the gas (e.g. collisional ionization, radiative recombination), together with those reactions involved in the formation and destruction of H_2 .

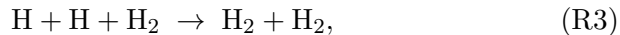
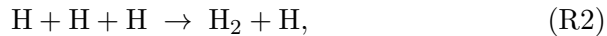
The formation of H_2 in local molecular clouds occurs primarily on the surface of interstellar dust grains: hydrogen atoms are adsorbed onto the surface of the grains, react to form H_2 and subsequently escape back into the interstellar medium (Gould and Salpeter, 1963). In primordial gas, however, there is no dust, and so no possibility of forming H_2 by this process. Instead, H_2 formation is dominated by various sets of gas phase reactions.

The simplest gas-phase reaction – direct radiative association of two hydrogen atoms to form H_2 :



is strongly forbidden unless one of the hydrogen atoms is in an excited electronic state, and therefore plays an important role only in rather unusual circumstances, such as in the intergalactic medium near the end of the epoch of recombination (Latter and Black, 1991; Rawlings, Drew, and Barlow, 1993). It does not significantly influence protogalactic H_2 formation.

Three-body formation of H_2 , via the reactions



can play a significant role (Palla, Salpeter, and Stahler, 1983), but only at high densities ($n_{\text{H}} \gtrsim 10^8 \text{ cm}^{-3}$), since the rate coefficients of these reactions are small. At lower densities, gas-phase formation of H_2 is dominated by two sets of reactions. The first involves the H^- ion as an intermediate state



and was first discussed in the context of the local ISM by McDowell (1961), and in a cosmological context by Peebles and Dicke (1968). The second set of reactions involves the H_2^+ ion as an intermediary, and was first discussed in a cosmological context by Saslaw and Zipoy (1967)



These two sets of reactions (hereafter the H^- pathway and the H_2^+ pathway respectively) share two important characteristics. Firstly, both are limited by their initial step, since the radiative association reactions R4 and R6 occur at a much slower rate than the subsequent ion-neutral reactions R5 and R7. Secondly, the role played by free electrons in the H^- pathway is extremely similar to the role played by H^+ ions in the H_2^+ pathway, and in both cases the H_2 formation rate is directly proportional to the fractional ionization of the gas, provided that the latter is small.²

The main difference between the two pathways stems from the difference in the rates of reactions R4 and R6: H^- forms via R4 much faster than H_2^+ forms via R6, and so the H^- pathway generally dominates the gas phase production of H_2 .

The dependence of H_2 formation on the presence of free electrons and protons might lead one to suppose that H_2 formation will be very inefficient in low temperature gas, since the equilibrium ionization fraction is very low. In practice, however, moderate amounts of H_2 can be formed if the protogalactic gas is not initially in ionization equilibrium. This is certainly the case in newly-formed protogalaxies, since the IGM itself is not in ionization equilibrium; instead, it retains a residual fractional ionization dating from the epoch of recombination. This comes about because the Hubble expansion ensures that the recombination timescale exceeds the expansion timescale before the IGM can reach equilibrium, freezing the fractional ionization at a value of approximately 2×10^{-4} (Stancil, Lepp, and Dalgarno, 1998). Protogalaxies forming from the IGM therefore begin with this small non-equilibrium fractional ionization.

Once a protogalaxy has formed, this residual ionization quickly vanishes, as the increased density leads to a greatly increased recombination rate. However, there remains a brief window of opportunity in which H_2 can form. Simple estimates of the resulting molecular fraction have been given by a number of authors (Susa *et al.*, 1998; Nishi

² If the fractional ionization is large, then the mutual neutralization of H^- with H^+ and the dissociative recombination of H_2^+ become significant, and this simple relationship breaks down; this is discussed in more detail in Glover (2003).

and Susa, 1999; Oh and Haiman, 2002) and are typically in the range $f_{\text{H}_2} = 10^{-3}$ – 10^{-4} . For comparison, note that the molecular fraction in the IGM at this time is approximately 2×10^{-6} (Galli and Palla, 1998).

Given the H_2 abundance, density and temperature, it is then a simple matter to calculate the H_2 cooling rate. Various parameterizations of this rate have been given in the literature; figure 2 shows some commonly cited examples, plotted as $\Lambda_{\text{H}_2}(n_{\text{H}}n_{\text{H}_2})^{-1}$, where Λ_{H_2} is the H_2 cooling rate per unit volume. The basic features of the cooling rate are straightforward: it falls off exponentially at low temperatures, due to the rather large excitation energy of the first accessible excited state (the $J = 2$ rotational state, which lies 512K above the $J = 0$ para-hydrogen ground state), and is essentially negligible below 100 K; it scales with density as $\Lambda_{\text{H}_2} \propto n_{\text{H}_2}^2$ at low densities, where radiative de-excitation dominates, and as $\Lambda_{\text{H}_2} \propto n_{\text{H}_2}$ at high densities, where collisional de-excitation dominates and the level populations approach their local thermodynamic equilibrium (LTE) values. The transition between low density and high density behaviour occurs near a critical density $n_{\text{cr}} \simeq 10^4 \text{ cm}^{-3}$.

The major uncertainty in the determination of the H_2 cooling rate comes from uncertainties in the values of the collisional de-excitation rates, which are highly sensitive to the details of the potential energy surface used to calculate them, as well as to the method of calculation adopted (Lepp, Buch, and Dalgarno, 1995). As a result, there exists substantial disagreement in the literature on the form and magnitude of the H_2 cooling rate at low densities, as can be seen from figure 2. However, recent calculations have removed much of this uncertainty, with the calculated collisional rates having more or less converged.

2.4. THERMAL EVOLUTION: SIMPLE MODELS

Armed with an appropriate set of chemical reaction rates and an accurate H_2 cooling rate (see, for example, Abel *et al.*, 1997 or Glover, 2001), the next step is to follow the coupled chemical, thermal and dynamical evolution of a protogalaxy as it forms in order to determine its fate.

The simplest approach to this problem dispenses entirely with any attempt to accurately simulate the dynamical evolution of the protogalaxy. Instead, the density evolution is specified in advance, and the model focuses on determining the chemical and thermal evolution of the gas. For instance, it is frequently assumed that if cooling is effective, then the density evolution will be the same as in pressure-free collapse. This approximation relies on the assumption that pressure gradients are everywhere small compared to gravitational forces.

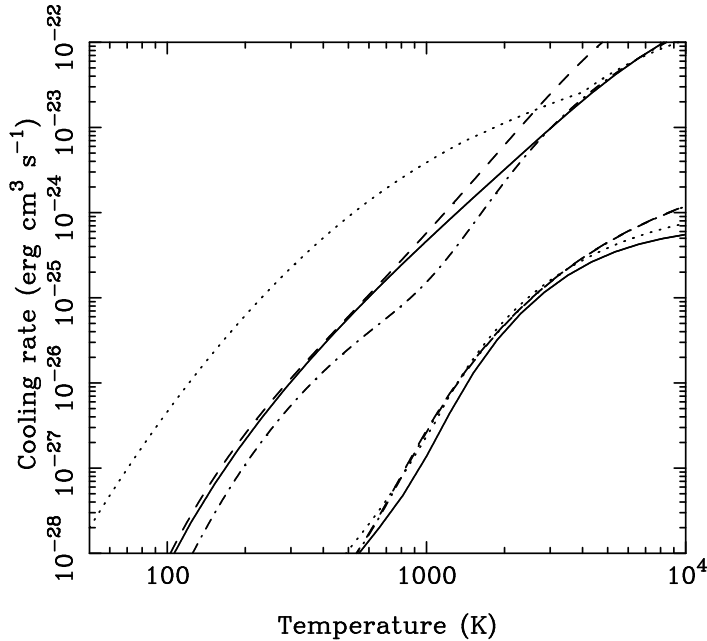


Figure 2. A comparison of various parameterizations of the H_2 cooling function, plotted in units of $\text{erg cm}^3 \text{s}^{-1}$. Rates are computed assuming that $n_{\text{H}} \gg n_{\text{H}_2}$, and that the ortho-to-para ratio is 3:1. The lower set of lines corresponds to a gas density $n_{\text{H}} = 10^6 \text{ cm}^{-3}$; the upper set corresponds to $n_{\text{H}} = 10^0 \text{ cm}^{-3}$. Solid line – Le Bourlot, Pineau des Forêts, and Flower (1999); dashed line – Galli and Palla (1998); dotted line – Lepp and Shull (1983); dash-dotted line – Hollenbach and McKee (1979).

A number of authors have considered the problem of protogalactic collapse within this framework (Matsuda, Sato, and Takeda, 1969; Hutchins, 1976; Yoshii and Sabano 1979, 1980; Carlberg, 1981; Palla, Salpeter, and Stahler, 1983; Villere and Bodenheimer, 1987; Susa, Uehara, and Nishi, 1996; Omukai, 2000; Flower and Pineau des Forêts, 2001), often supplementing it with the additional assumptions of spherical symmetry and uniform density. Use of these approximations reduces the problem to one of computing the chemical and thermal evolution of a single representative parcel of gas.

Most of these models predict the same general type of behaviour. Initially, the H_2 cooling rate is negligible and the evolution of the gas is very close to adiabatic. As the collapse proceeds, however, the increasing temperature, density and H_2 abundance all combine to dramatically increase the H_2 cooling rate and decrease t_{cool} . Eventually, t_{cool} becomes comparable to the collapse timescale, and the collapse ceases to be even approximately adiabatic. Instead, the temperature reaches a peak and then decreases at higher densities as radiative cooling becomes

increasingly dominant over compressional heating. The quantitative details, such as the value of the peak temperature, are sensitive to the treatment of H_2 cooling and gas chemistry adopted, and generally vary from model to model, although never by more than a factor of a few.

The only case in which this type of model predicts substantially different behaviour is when some other process, such as UV photodissociation, acts to reduce the H_2 abundance (see, e.g. Omukai, 2001). In this case, the protogalaxy may be unable to form sufficient H_2 to cool the gas before it reaches a temperature and density at which collisional dissociation of H_2 becomes significant. This results in the gas temperature continuing to rise until the onset of Lyman- α cooling at a temperature of approximately 10^4 K.

An alternative model is presented by Tegmark *et al.* (1997). They make a similar set of approximations (spherical symmetry, uniform density, free-fall collapse), but halt the collapse when one of two conditions is met:

- (i) The gas temperature exceeds the virial temperature of the protogalaxy, defined as (Blanchard, Valls-Gabaud, and Mamon, 1992):

$$T_{\text{vir}} = \frac{GM\mu m_{\text{H}}}{2kR_{\text{vir}}}. \quad (16)$$

- (ii) The mean density of the gas exceeds the mean density of the dark matter halo. The latter can be written as

$$\bar{\rho}_{\text{DM}} = (1 + \Delta)\rho_{\text{dm}}, \quad (17)$$

where $\Delta = 18\pi^2$ for an Einstein-de Sitter cosmology (Peebles, 1980); analogous values for open or Λ -dominated cosmological models are given in Bryan and Norman (1998).

If condition (ii) is met, then shocks are assumed to raise the gas temperature instantaneously to T_{vir} at the end of the collapse.

Tegmark *et al.* (1997) make no attempt to follow the further dynamical evolution of the gas. Instead, they hold its density constant, and study its subsequent thermal and chemical evolution. If the gas temperature decreases by more than 25% during an interval corresponding to a 25% decrease in redshift, i.e. if

$$T(0.75z_c) \leq 0.75T(z_c), \quad (18)$$

where z_c is the redshift at which the collapse terminates, then the protogalaxy is considered to be able to cool effectively. Otherwise, cooling is considered to be ineffective.

By performing this analysis for protogalaxies with a wide range of masses and collapse redshifts, Tegmark *et al.* are able to map out the region in M - z_c parameter space corresponding to protogalaxies that can cool effectively. They find that at each redshift they can identify a minimum mass M_{\min} such that protogalaxies with $M > M_{\min}$ cool effectively, while those with $M < M_{\min}$ do not. For instance, at $z = 30$, they find that $M_{\min} \sim 10^6 M_{\odot}$, two orders of magnitude larger than the Jeans mass at that redshift. This result can also be expressed in terms of a minimum virial temperature, T_{\min} , related to M_{\min} through Equation (16); at $z = 30$, this is 1000 K. While the values of M_{\min} and T_{\min} obtained in this way are somewhat sensitive to the choice of H_2 cooling function (Abel *et al.*, 1998; Glover, 2001), the basic behaviour remains the same.

These two approaches – the free-fall collapse model and the Tegmark *et al.* model – therefore present us with two distinct scenarios for the formation of protogalaxies. The free-fall models predict that every protogalaxy can cool, with the onset of cooling occurring once the gas has reached a temperature of approximately 1000 K (give or take a factor of two). On the other hand, the Tegmark *et al.* model predicts that only those protogalaxies with $T_{\text{vir}} > 1000$ K will cool; smaller protogalaxies, with lower virial temperatures, will simply remain as pressure-supported gas clouds and will not form stars.

Are either of these scenarios correct? Ultimately, this depends upon whether the approximations on which they are based are justified. This is a question that is best addressed through the use of more detailed numerical simulations.

2.5. THERMAL EVOLUTION: NUMERICAL SIMULATIONS

The biggest problem that we face when trying to simulate protogalactic collapse numerically is the wide range of length scales that we are required to resolve. For example, consider the collapse of a $10^6 M_{\odot}$ protogalaxy. This has a characteristic size (as given by the virial radius) of approximately 3 kpc in comoving units, corresponding to 100 pc in physical units at $z = 30$. To properly simulate its cosmological environment, we should follow the evolution of the gas and dark matter on scales that are two to three orders of magnitude larger (see, for instance, the resolution study of Ricotti, Gnedin, and Shull, 2002a), while to resolve star formation within it, we need to be able to follow the gas down to scales of the order of an AU. The total dynamical range required in order to resolve all of this within a single simulation is therefore approximately 10^{10} , many orders of magnitude larger than can be covered with a single fixed grid.

The simplest way in which we can obtain the required dynamical range is to use a Lagrangian grid, i.e. one which moves with the fluid flow. This is particularly effective if one assumes that protogalaxies are spherically symmetric, as in this case we can use a simple one-dimensional Lagrangian code, such as that described by Thoul and Weinberg (1995).

The earliest studies of this type were performed by Peebles and Dicke (1968) and Pöppel (1975), but the initial conditions that they adopted – isolated, isothermal clouds, initially in hydrostatic equilibrium – are not appropriate for protogalaxies forming by dynamical collapse within an expanding cosmological model. More recent simulations by Haiman, Thoul, and Loeb (1996), Oliveira *et al.* (1998ab) and Stachniewicz and Kutschera (2003) begin from more appropriate cosmological initial conditions and all three groups obtain broadly similar results.

The most significant result of these simulations is the demonstration that the dynamical evolution of a small, H_2 cooled protogalaxy is *not* well described by pressure-free gravitational collapse. Instead, pressure plays a important role, particularly for protogalaxies with masses near M_J . It has two main effects. In the initial stages of collapse, when the flow is subsonic, it delays the collapse of the gas relative to the dark matter, resulting in a density profile which is less centrally concentrated than would otherwise be the case. At a later time, once the infall has become supersonic, the finite pressure leads to the formation of an accretion shock near the virial radius of the halo. The majority of the H_2 that forms does so in the post-shock gas, and it is the conditions there that determine whether or not the protogalaxy is able to cool effectively (Haiman, Thoul, and Loeb, 1996).

Of the two scenarios discussed in the previous section, the Tegmark *et al.* model clearly provides the better description. The major point of disagreement is the protogalactic density profile: for simplicity, Tegmark *et al.* assume a uniform density profile, while the simulation results show that the true profile is much closer to that of an isothermal sphere.

Unfortunately, one-dimensional Lagrangian simulations, although simple to perform and quick to run, ultimately give us a rather limited view of protogalactic formation, since they do not include many important physical effects such as rotation and turbulence. To identify the role that these factors play, we need to use fully three-dimensional hydrodynamical simulations.

The move to three dimensions necessitates a change in our computational strategy, as grid-based Lagrangian codes do not handle three dimensional flows well due to the severe grid distortion that tends to occur and which causes a dramatic loss of accuracy. This problem can be circumvented to some degree through the use of ‘hybrid’ codes,

which switch to Eulerian (i.e. fixed) coordinates in regions of high deformation. Examples include the codes of Gnedin (1995; see also Gnedin and Bertschinger, 1996) and Pen (1998). However, although this technique has been used to study protogalactic feedback (Ostriker and Gnedin, 1996; Gnedin and Ostriker, 1997; Ricotti, Gnedin, and Shull, 2002ab), it has not been used to study primordial star formation in any detail.

Another way to avoid the grid distortion problem is to abandon the use of a grid, and to switch to a particle-based Lagrangian technique such as smoothed particle hydrodynamics (SPH; see Gingold and Monaghan, 1977; Lucy, 1977; Monaghan, 1992). Alternatively, the required dynamical range can be obtained using fixed grids if multiple nested grids, or some form of grid refinement are used. Both of these approaches are discussed in more detail below.

2.5.1. SPH simulations

Several authors have studied the formation of protogalaxies using SPH (Bromm, Coppi, and Larson, 1999, 2002; Fuller and Couchman, 2000; Yoshida *et al.*, 2003). Fuller and Couchman (2000) used the HYDRA cosmological SPH code (Couchman, Thomas, and Pearce, 1995) to study the collapse of uniform, spherical protogalaxies of various masses at a range of different redshifts, in order to test the predictions of Tegmark *et al.* (1997). They obtained broadly similar results, although their values of T_{\min} are roughly a factor of two smaller than those of Tegmark *et al.*, a discrepancy which may simply be due to the different H_2 cooling functions used in the two studies.

Fuller and Couchman also studied protogalactic formation in a more realistic cosmological simulation. They demonstrated that the evolution of the most massive object in their simulations could be divided into two main phases. In the first phase, the halo mass is less than the Jeans mass, pressure forces dominate, and the baryonic overdensity is small, but non-zero. This phase corresponds to the delayed collapse phase seen in the one-dimensional simulations discussed above.

During this phase, the mass of the halo continues to increase, driven to a large extent by mergers with smaller dark matter halos. As the mass nears M_J , the gas density profile begins to steepen significantly as gravitational forces become dominant. At this stage, the gas temperature is already significantly higher than the temperature of the IGM, while the fractional H_2 abundance in the central dense region is of order 10^{-4} , two orders of magnitude larger than its initial value. Nevertheless, the cooling time remains longer than the dynamical timescale, and the gas is not yet self-gravitating.

The second phase begins once t_{cool} drops below t_{dyn} at the centre of the protogalaxy. The central gas rapidly cools to $T \sim 150$ K, and the consequent reduction in pressure support leads to a substantial increase in the central density. The gas eventually becomes self-gravitating at $z \simeq 20$, at which point the protogalaxy has a mass $M \simeq 4 \times 10^5 M_{\odot}$, close to the estimate of M_{min} at that redshift.

Inspection of the spherically averaged temperature and density profiles of the protogalaxy allows us to identify several distinct regions. From the outside in, we have:

- (i) Cosmological infall, terminated by an accretion shock
- (ii) A broad, post-shock region, where heating from adiabatic compression competes with H_2 cooling, and where $t_{\text{cool}} > t_{\text{dyn}}$
- (iii) A cold, dense central core, where $t_{\text{cool}} < t_{\text{dyn}}$.

Unfortunately, the structure of the core region is not well resolved in Fuller and Couchman’s simulation, since its extent is comparable to the minimum smoothing length of their SPH code.

Bromm, Coppi, and Larson (1999, 2002) simulated protogalactic collapse using a modified version of the TREESPH code (Hernquist and Katz, 1989). They concentrated on following in detail the evolution of a single protogalaxy and consequently adopted simplified initial conditions: a spherical overdensity, set into rigid rotation with a specified angular momentum and perturbed on small scales using the Zeldovich approximation (Zeldovich, 1970) with a $P(k) \propto k^{-3}$ power spectrum. By focusing on a single protogalaxy and neglecting its cosmological environment, they were able to follow its collapse to high densities ($n \leq 10^8 \text{ cm}^{-3}$). On large scales, their results confirm those of Fuller and Couchman (2000): the gas initially evolves adiabatically, is heated up to $T \sim T_{\text{vir}}$ in an accretion shock, and subsequently cools to $T \sim 100\text{--}200$ K in the dense central regions. On small scales, their greater resolution allowed them to follow the formation of structure within the dense, cold gas. This portion of their results is discussed in detail in section 3.

Finally, Yoshida *et al.* (2003) used the GADGET code (Springel, Yoshida, and White, 2001) to explore the cosmological environment in which the first protogalaxies form. They performed the largest protogalactic simulation to date, using 48 million SPH particles to simulate the evolution of a cosmological volume which is $600h^{-1}$ comoving kiloparsecs on a side. This simulation had a mass resolution of approximately $5000h^{-1} M_{\odot}$ and a spatial resolution of approximately $50h^{-1}$ pc, and so resolved little of the internal structure of the protogalaxies.

On the other hand, it did allow a large sample of protogalaxies to be studied within a single consistent simulation, and was therefore a useful complement to more detailed studies of single protogalaxies.

Yoshida *et al.* found that to cool efficiently, protogalaxies in their simulation must have masses $M \simeq 5 \times 10^5 h^{-1} M_{\odot}$, and fractional H_2 abundances $f_{\text{H}_2} \simeq 2 \times 10^{-4}$. Moreover, while all of the protogalaxies with large H_2 abundances also had large masses, the converse was not true; some protogalaxies with masses above $5 \times 10^5 h^{-1} M_{\odot}$ did not form enough H_2 to cool. Further investigation of these protogalaxies showed that they were gaining mass more rapidly than their cooler counterparts, leading Yoshida *et al.* to suggest that their temperatures were being kept high by the compressional heating associated with frequent merger activity. If this is the case, then it implies that the ability of a particular protogalaxy to cool and form stars depends on its dynamical history as well as its current mass. Further investigation of this point is clearly warranted.

2.5.2. Multigrid simulations

The basic idea behind a multiple grid (or multigrid) Eulerian simulation is to take a single top-level grid that is large enough to represent the whole volume of interest, and then to supplement it with one or more levels of subgrids in regions in which higher resolution is desired. Since much of the volume of a typical cosmological simulation is filled with under-dense material that is well resolved by the top-level grid alone, this technique can dramatically improve the dynamical range of an Eulerian simulation for only a small increase in its computational cost.

In the simplest implementation of the multigrid technique, the placement of the grids is specified at the beginning of the simulation and does not subsequently alter. This is the approach used in the protogalactic simulations of Abel *et al.* (1998). They used the HERCULES code (Anninos, Norman, and Clarke, 1994; Anninos *et al.*, 1997) to study the growth of 3σ and 4σ density peaks within a large cosmological volume. The simulations were performed using a top-level grid with a resolution of 128^3 , together with a quarter-size subgrid with the same resolution, for an effective resolution of 512^3 . The initial conditions were arranged to ensure that the density peak would remain within the region covered by the subgrid.

These simulations were able to resolve the basic filamentary structure of the IGM surrounding the protogalaxies, and gave some indications that gas cooling within the protogalaxies was not particularly efficient. However, the protogalaxies remained under-resolved, rendering these conclusions uncertain.

A natural way to improve the resolution would be to add more subgrids. However, as one does this, it becomes increasingly difficult to ensure that the subgrids are placed correctly, since at the beginning of the simulation it is generally not possible to determine exactly which regions will require very high resolution. Fortunately, this problem can be overcome by the use of a technique called adaptive mesh refinement.

In an adaptive mesh simulation, the placement of subgrids is not specified a priori. Instead, one or more refinement criteria are specified, and local subgrids are created as required to ensure that these criteria are always satisfied. Adaptive mesh codes have been used with great success in a number of areas of astrophysics, as discussed in the recent review of Norman (2004). Their use in the study of primordial star formation was pioneered by Abel, Bryan, and Norman (2000, 2002) in a pair of highly influential papers.

In the first of these papers, Abel, Bryan, and Norman (2000) used the ENZO code of Bryan and Norman (1997ab) to follow the evolution of protogalactic gas from cosmological scales down to densities of order 10^6 cm^{-3} . They achieved a maximum resolution of 0.4 pc (in comoving units) within a box that was 128 comoving kpc on a side, for a total dynamic range of approximately 3×10^5 . This simulation produced a protogalaxy with the same basic temperature profile as found in the SPH simulations: a cold infall region, an accretion shock at $r \sim r_{\text{vir}}$, a subsequent broad cooling zone, and a cold, dense central region. In a subsequent simulation, described in Abel, Bryan, and Norman (2002), they included additional molecular physics (the three-body formation of H_2) and followed the collapse to significantly higher densities, eventually reaching a minimum physical resolution of a few tens of AU.

Although Abel, Bryan, and Norman present many of their results, such as the temperature and density profiles, in the form of spherically averaged quantities, they also present a number of slices through their simulations on different scales. These demonstrate that the assumption of spherical symmetry is a relatively crude approximation, particularly on large scales, since much of the gas falling into the potential well of the protogalaxy does so along a few overdense filaments, rather than in a spherically symmetric fashion.

The very high dynamical range achieved in their simulations also allowed Abel, Bryan, and Norman to study in detail the evolution of the dense gas at the centre of the simulated protogalaxy. This portion of their results is discussed later, in section 3.

2.6. SUMMARY

By combining the detailed results of the numerical simulations described in the previous section with the more general theoretical considerations of sections 2.1–2.4, we are able to put together a reasonably comprehensive answer to the first of the questions posed in the introduction: when do the first protogalaxies form, and how large are they?

As we have seen, the earliest protogalaxies will form at a redshift of 30–40, and will have masses of order $10^4 M_\odot$. However, these protogalaxies will form little H_2 and will not be able to cool effectively. They are therefore extremely unlikely to form stars. The earliest star-forming protogalaxies will form later, at $z \sim 30$, and will be more massive, with masses of order 10^5 – $10^6 M_\odot$, and virial temperatures of order 1000 K.

Finally, it should be noted that these results assume a CDM-based cosmological model. If this turns out to be an incorrect description of dark matter on small scales, then we should expect these numbers to change significantly. For instance, if some form of warm dark matter is a more appropriate description, then the first protogalaxies will be larger ($M \sim 10^7 M_\odot$) and will form at lower redshift ($z \sim 20$), as demonstrated in the recent simulation by Yoshida, Sokasian, Hernquist, and Springel (2003). However, models such as this have great difficulty accounting for the high electron scattering optical depth detected by WMAP (Kogut *et al.*, 2003), and at present there seems little reason to prefer them over CDM.

3. Fragmentation

Once we have established that a significant amount of protogalactic gas can cool and condense on a cosmologically interesting timescale, the next step is to investigate what happens to this gas. In particular, we would like to know whether any of it forms stars, and, if so, how many stars form, over what timescale, and with what IMF?

Crucial to determining this is an understanding of the degree to which the protogalactic gas fragments during its dynamical evolution: does the cold gas sink into the centre of the halo, forming a single massive clump? Or does it break up into many smaller clumps? To address these questions, in the following sections I examine the effectiveness of the various mechanisms that may bring about fragmentation, and discuss the results of the most recent numerical investigations.

3.1. HIERARCHICAL FRAGMENTATION

An obvious place to begin is with the force responsible for the formation of the protogalaxy itself: *gravity*. For gravitational fragmentation to be effective, two important conditions must be met. First, any fragments that form must be gravitationally bound. Second, regions that begin to collapse due to their own self-gravity must be able to complete this collapse on a timescale shorter than the dynamical timescale of the flow in which they are embedded; otherwise, they will be disrupted before they have time to grow into distinct objects.

The question of whether a particular fragment is gravitationally bound depends, in the general case, on a number of factors: the mass of the fragment, its internal velocity field and pressure distribution, the properties of the surrounding gas flow etc. (see McKee and Zweibel, 1992 for a detailed discussion). However, much of the work done on gravitational fragmentation in a primordial context makes the simplifying assumptions that the only forces acting are gravity and pressure, and that the latter can be neglected on scales larger than the Jeans length. Although the validity of these assumptions is questionable, they provide a simple starting point for an investigation of protogalactic fragmentation, so I will briefly discuss the conclusions they lead us to, before going on to consider more detailed models.

My starting point is the work of Hoyle (1953). He considered the gravitational collapse of a homogeneous protogalaxy, and showed that on scales where pressure can be neglected, the second of our conditions for fragmentation will always be satisfied. His argument is very simple: gas with a density ρ collapses gravitationally on a timescale $t_{\text{ff}} \propto (G\rho)^{-1/2}$, while a perturbed region with a density ρ' will collapse on a timescale $t'_{\text{ff}} \propto (G\rho')^{-1/2}$. If $\rho' > \rho$, then $t'_{\text{ff}} < t_{\text{ff}}$, and so the perturbed region will collapse faster than the main flow. In the protogalactic case, this implies that overdense regions within the protogalaxy will be able to collapse under their own self-gravity in less time than it takes for the protogalaxy itself to collapse. Therefore, the protogalaxy will fragment.

Hoyle also pointed out that one can apply precisely the same argument to every fragment that forms within the protogalaxy: provided that they contains overdense regions, and that the neglect of pressure forces remains appropriate, they too will fragment (as will the fragments of these fragments etc.). Hoyle therefore argued that the protogalactic gas would continue to fragment on smaller and smaller scales until pressure forces finally intervened to prevent further fragmentation, a scenario that has come to be known as *hierarchical fragmentation*.

Hoyle’s original semi-quantitative argument was subsequently placed on a sounder mathematical basis by Hunter (1962), who performed a linear perturbation analysis of a uniform, spherical, pressure-free collapse and showed that any overdense perturbation would be gravitationally unstable and would quickly grow until it became nonlinear in less than a free-fall time. Hunter (1964) expanded on this analysis by considering second order terms and showed that these would accelerate the growth of overdense regions. Similar analyses have also been made by Savedoff and Vila (1962) and Silk (1982), with similar results.

3.2. THE OPACITY LIMIT

An important prediction of the hierarchical fragmentation scenario is that the smallest fragments will have sizes of the order of the Jeans length, and hence masses of the order of the Jeans mass, since this is the scale on which pressure balances gravity. However, both λ_J and M_J are functions of the density and temperature of the gas, and will change as the protogalaxy evolves. To identify the minimum fragment mass, we must therefore determine how small M_J becomes during the collapse.

Recall that we can write M_J in terms of the gas density as

$$M_J \propto \rho^{\frac{3}{2}(\gamma_{\text{eff}} - \frac{4}{3})}, \quad (19)$$

where the effective adiabatic index γ_{eff} is

$$\gamma_{\text{eff}} = 1 + \frac{d \ln T}{d \ln \rho}. \quad (20)$$

For $\gamma_{\text{eff}} < 4/3$, the Jeans mass decreases with increasing density, while for $\gamma_{\text{eff}} > 4/3$ it increases. Hoyle (1953) suggested that a transition from $\gamma_{\text{eff}} < 4/3$ to $\gamma_{\text{eff}} > 4/3$ would occur when the gas first became optically thick, under the assumption that this would mark a change from isothermal evolution to adiabatic evolution. The density and temperature of the gas at this time would then set the minimum fragment mass. This basic idea – that it is the opacity of the gas which sets a lower limit on the mass of a fragment and therefore on the mass of a star – has become known as *opacity-limited fragmentation*, and has been studied by a number of authors.

Low and Lynden-Bell (1976) and Silk (1977b) both follow Hoyle in assuming that the minimum mass is reached at the moment that a fragment first becomes optically thick. They also assume that the fragment is in thermal balance at this time, with compressional heating balanced by radiative cooling. These assumptions provide them with

two equations relating T_F , ρ_F and κ_F (the temperature, density and opacity of the fragment at the moment that it becomes optically thick):

$$\kappa_F \rho_F \frac{\lambda_J(\rho_F, T_F)}{2} = 1, \quad (21)$$

$$\Gamma_c(\rho_F, T_F) = \Lambda_r(\rho_F, T_F, \kappa_F), \quad (22)$$

where Γ_c is the compressional heating rate and Λ_r is the radiative cooling rate.

We can use these equations to express the minimum fragment mass M_F in terms of a single unknown – for instance, Low and Lynden-Bell (1976) write it in terms of the opacity as

$$M_F = 2.5 \times 10^{-3} \mu^{-16/7} \left(\frac{\kappa_0}{\kappa_F} \right)^{1/7} M_\odot, \quad (23)$$

where μ is the mean molecular weight and κ_0 is the opacity due to Thomson scattering – but to fully determine M_F , we need an additional piece of information. In Hoyle’s original analysis, this comes from the assumption that the radiative cooling is dominated by Lyman- α emission, which fixes the temperature at approximately 10^4 K. On the other hand, Silk (1977b) considers a case where the cooling and opacity are both dominated by dust, in which case the observed dust temperature provides the additional information required. In general, however, we can only determine M_F if we know something of the previous thermal history of the gas.

Rees (1976) studied the opacity limit from a different viewpoint, arguing that the essential requirement for continued isothermal evolution is that a fragment be able to radiate away its gravitational binding energy in less than a free-fall time, and that opacity is only important inasmuch as it limits the maximum radiative rate, which cannot exceed that of a black body of a similar temperature. This fact can be used to derive the minimum temperature that a fragment must have in order to radiate sufficient energy, which in turn can be used to determine M_F :

$$M_F = M_c \mu^{-9/4} f^{-1/2} \left(\frac{kT_F}{m_p c^2} \right)^{1/4}, \quad (24)$$

where M_c is the Chandrasekhar mass, m_p is the mass of a proton and f is a radiative efficiency factor, defined as the ratio of the actual radiation rate to the black-body rate:

$$f = \frac{\int F_\nu d\nu}{\int \pi B_\nu d\nu}. \quad (25)$$

From Equation (24), we see that if $f \sim 1$, then M_F will be of the order of a solar mass (or less, if T_F is very small), while if $f \ll 1$, as may occur if the cooling is dominated by a few narrow emission lines, then M_F may be of the order of tens or hundreds of solar masses.

More recently, Masunaga and Inutsuka (1999) have reconsidered the conditions under which isothermal evolution comes to an end. They show that this will inevitably occur once the radiative cooling rate becomes unable to keep pace with the compressional heating rate, and that this may take place in either the optically thin or optically thick regime, depending on the details of the collapse, but is unlikely to coincide with the instant at which $\tau = 1$. This suggests that a better procedure for determining M_F is to follow the actual thermal evolution of the gas.

3.3. SIMPLE NUMERICAL MODELS

Various authors have attempted to calculate M_F by modelling the thermal evolution of the collapsing protogalactic gas. One of the earliest was Yoneyama (1972), who constructed an evolutionary track for the gas in density-temperature space by assuming that it always satisfied the following conditions:

$$t_{\text{cool}} = t_{\text{ff}}, \quad (26)$$

$$t_{\text{H}_2} = \max(t_{\text{ff}}, t_{\text{rec}}), \quad (27)$$

where t_{H_2} is the H_2 formation timescale, given by

$$t_{\text{H}_2} = \frac{n_{\text{H}_2}}{k_{\text{H}^-} n_{\text{e}} n_{\text{H}}}, \quad (28)$$

where k_{H^-} is the rate coefficient for the formation of H^- by radiative association of electrons and H I (reaction R4), and t_{rec} is the recombination timescale, given by

$$t_{\text{rec}} = \frac{1}{k_{\text{rec}} n_{\text{H}^+}}, \quad (29)$$

where k_{rec} is the rate coefficient for radiative recombination. Yoneyama used this technique to calculate the evolution of M_J until either the gas became optically thick or became hot enough to collisionally dissociate H_2 . M_F could then be computed simply by finding the minimum value of M_J reached along the evolutionary trajectory. Yoneyama found that in small protogalaxies, the minimum value was reached shortly before the gas became hot enough to collisionally dissociate H_2 and that $M_F \simeq 60 M_{\odot}$; in larger protogalaxies, the greater column density of H_2 caused

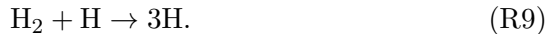
the gas to become optically thick before collisional dissociation could occur, and the resulting value of M_F was considerably larger.

A more common approach is to specify the form of $\rho(t)$ in advance, often by constructing some extremely simplified dynamical model for the protogalaxy, and then to use this as an input into a more detailed chemical and thermal model. Many such models exist (Hutchins, 1976; Silk, 1977a; Carlberg, 1981; Hasegawa, Yoshii, and Sabano, 1981; Palla, Salpeter, and Stahler, 1983; Lepp and Shull, 1984; Lahav, 1986; Villere and Bodenheimer, 1987; de Araujo and Opher, 1989; Susa, Uehara, and Nishi, 1996); I will discuss only a few notable examples.

Hutchins (1976) studied the thermal evolution of a variety of spherical and spheroidal protogalaxies using a very simplified chemical model consisting of only four reactions – formation of H_2 via the H^- pathway (reactions R4–R5), plus radiative recombination of hydrogen



and collisional dissociation of H_2 by H:



His cooling function was equally simple, and included only Compton cooling and H_2 rotational cooling. The calculations were terminated once H_2 dissociated. Hutchins found a minimum fragment mass of approximately $200 M_\odot$, within a factor of a few of Yoneyama’s result.

Silk (1977a) and Carlberg (1981) both investigated the effects of including Lyman- α cooling in the model, and showed that it has a dramatic effect. The reason is that the collisional dissociation of H_2 no longer results in a permanent transition to adiabatic evolution. Instead, the gas heats up adiabatically for a short while, until its temperature reaches 10^4 K, following which it again begins to evolve isothermally. This second phase of isothermal evolution is eventually terminated once the fragments become optically thick in the continuum. It allows M_F to reach much smaller values than would otherwise be possible. Silk (1977a) estimated the minimum fragment mass to be approximately $0.3 M_\odot$; Carlberg (1981), using a more detailed treatment, found $M_F \sim 0.5 M_\odot$.

Finally, Palla, Salpeter, and Stahler (1983) investigated the importance of three-body H_2 formation (reactions R2–R3) and showed that at high densities ($n > 10^8 \text{ cm}^{-3}$), these reactions become very effective, rapidly converting the bulk of the hydrogen to molecular form. This dramatically increases the H_2 cooling rate, delaying the collisional dissociation of H_2 until much higher densities are reached, and consequently lowers M_F . For the representative example of a $5 \times 10^4 M_\odot$

cloud, Palla, Salpeter, and Stahler (1983) found a minimum fragment mass of $M_F \sim 0.1 M_\odot$.

The main lesson to draw from these attempts is the importance of an accurate treatment of the thermal evolution of the gas, which requires a comprehensive treatment of the microphysics – comparison of the results of Hutchins (1976) with those of Silk (1977a) or Palla, Salpeter, and Stahler (1983) demonstrates the danger of using an oversimplified chemical or thermal model. However, the specific predictions of these models rely upon the accuracy of the assumptions made regarding the density evolution, and we have already seen that simple collapse models generally do not perform well in this respect. More importantly, these predictions rely on the correctness of the basic assumptions underlying the hierarchical fragmentation scenario. Unfortunately, there are good reasons to believe that these assumptions are not correct, as I discuss in the next section.

3.4. THE CASE AGAINST HIERARCHICAL FRAGMENTATION

Recall that the hierarchical fragmentation scenario is based on two major assumptions: first, that the balance between gravity and pressure is the only determinant of whether a fragment is gravitationally bound, and second, that the gas flow on scales larger than the Jeans length can be approximated by pure gravitational free-fall. The first of these assumptions implies that all fragments with $M > M_J$ will be gravitationally bound; the second, that the gas can quickly fragment down to the Jeans scale, provided that it starts from moderately uniform initial conditions. Clearly, both of these assumptions represent substantial simplifications. However, the real question is whether the simplified picture remains accurate; in other words, did hierarchical fragmentation actually occur in real protogalaxies?

One important argument against this scenario was first advanced by Layzer (1963). He argued that as the protogalactic gas fragmented, the individual fragments would tend to acquire angular momentum from the gravitational torques exerted on them by their neighbours. If this angular momentum was subsequently conserved during the evolution of the fragment, then it would limit the extent to which it could contract, and would help to stabilize it against further fragmentation.

A convenient way to parameterize this is in terms of the dimensionless spin parameter

$$\lambda \equiv \frac{J|E|^{1/2}}{GM^{5/2}} \simeq \frac{v_{\text{rot}}}{v_{\text{ff}}}, \quad (30)$$

where J and E represent the fragment's total angular momentum and total energy respectively. If angular momentum is conserved, then the

fragment’s rotational velocity will scale as $v_{\text{rot}} \propto R^{-1}$ (where R is the size of the fragment), and since its free-fall velocity will scale as $v_{\text{ff}} \propto R^{-1/2}$, this implies that $\lambda \propto R^{-1/2}$; in other words, the fragment will spin faster as it contracts. The fragment will become centrifugally supported once $\lambda = 1$, and so the contraction of the fragment will stop once it reaches a size

$$R = \lambda_0^2 R_0 \quad (31)$$

where λ_0 is the initial spin parameter of the fragment, and R_0 is its initial size.

Layzer (1963) estimated the initial spin parameter to be of order unity, and therefore argued that any fragments that formed would be barely distinct from the background gas, and would inevitably collide and coalesce before the end of the protogalactic collapse. Hunter (1964), however, disagreed and argued that the mutual gravitational torques between the fragments would not affect their spins. He noted that in a freely-falling, isothermal, inviscid gas, Kelvin’s circulation theorem would apply, and so therefore the vorticity of a fragment would change only due to its expansion or contraction; the gravitational field would have no direct effect. In this analysis, Equation (31) still applies, but λ_0 depends purely on the initial vorticity of the gas forming the fragment, and is substantially less than one.

Regardless of the correct value of λ_0 , it is clear from this analysis that at some point the fragments will become centrifugally supported, provided that they conserve angular momentum. Once this occurs, the assumption of free-fall collapse made by Hoyle, Hunter and many others is clearly no longer appropriate. Moreover, centrifugally supported fragments will tend to flatten into rotating disks, which have different stability properties from those of collapsing spheres, as discussed at some length in Larson (1985). Specifically, one can define a parameter

$$Q = \frac{c_s \kappa}{\pi G \mu} \quad (32)$$

where κ is the epicyclic frequency of the disk and μ is its surface density, such that disks with $Q > Q_{\text{crit}}$ are stable against gravitational fragmentation³. The value of Q_{crit} depends to some extent on the equation of state of the gas, but typically $Q_{\text{crit}} \sim 0.5\text{--}0.6$ (Goldreich and Lynden-Bell, 1965; Larson, 1985). Furthermore, even if the first generation of centrifugally supported fragments remain unstable (i.e. if they have $Q < Q_{\text{crit}}$), subsequent generations will be more highly stabilized (Larson 1984, 1985), provided that the evolution is isothermal.

³ Note that this Q is analogous to the Toomre (1964) stability parameter for a stellar disk.

Therefore, rather than the successive fragmentation envisioned in the hierarchical fragmentation scenario, one may instead find only one or two generations of fragments form, with rotation quickly acting to suppress fragmentation on smaller scales.

Another serious critique of the hierarchical fragmentation scenario was put forward by Tohline (1980). He pointed out that there is a fundamental difference between the growth of perturbations in a pressure-free collapse, such as that considered by Hunter (1962), and in a pressurized collapse. In a pressure-free collapse, overdensities are gravitationally unstable on *all* scales, and begin to grow immediately. In a pressurized collapse, on the other hand, only overdensities with masses larger than the initial Jeans mass can grow to begin with. Although smaller overdensities will subsequently become unstable and begin to grow as M_J decreases during the protogalactic collapse, the onset of their growth is delayed. This effect is particularly pronounced if the initial Jeans mass is close to the mass of the protogalaxy, as in this case small perturbations will be unable to grow until after the protogalaxy has already collapsed by a significant amount.

Based on this, Tohline argued that one of the fundamental assumptions of the hierarchical fragmentation scenario – the rapid fragmentation of the gas down to scales of order of the Jeans mass – is not correct, since M_J may vary faster than the gas can respond. In particular, he argued that the minimum mass of a fragment at the time that the gas becomes optically thick will not be equal to the Jeans mass at that moment, since overdensities with $M \sim M_J$ will only just have become unstable, and will not yet have had the chance to grow. Instead, the minimum fragment mass will correspond to the Jeans mass at some earlier time, and will therefore be significantly larger than is predicted by the models discussed in the previous section.

Another way to consider this issue is to examine the dispersion relation arising from the perturbation analysis. For the classical Jeans analysis of plane wave density perturbations in an infinite uniform medium, one obtains

$$\omega^2 = c_s^2 k^2 - 4\pi G\rho, \quad (33)$$

and the same relation holds for spherically symmetric density perturbations of the form $r^{-1}\sin kr$ (Larson, 1985). In the pressure-free case, $c_s = 0$, and the growth rate of perturbations is scale-free. On the other hand, in the pressurized case, c_s is non-zero and the growth rate increases with decreasing wavenumber, reaching a maximum for $k = 0$. In other words, large-scale perturbations grow faster than small-scale perturbations, suggesting that for the latter to win out and to cause fragmentation to occur, they must start with substantially higher densities. Although Equation (33) applies directly only to a rather idealized

protogalaxy, it is reasonable to expect to find similar behaviour in the more general case.

A final problem with the hierarchical fragmentation scenario is that it assumes that the gas is initially uniform (which implies that t_{ff} is the same everywhere), and remains so during the collapse. However, this is unlikely to be the case. Even if the gas begins its collapse from a uniform state, it will tend to become centrally concentrated during the course of the collapse (Bodenheimer and Sweigart, 1968; Larson, 1973; Tohline, 1982) as a pressure gradient builds up between the centre and the edge of the protogalaxy. This is significant, because a centrally concentrated gas cloud is far more stable than a uniform cloud with regard to the growth of small self-gravitating perturbations, as a number of authors have demonstrated (Army, 1966; McNally and Settle, 1980; Silk and Suto, 1988; Lacey, 1989). Although many of these analyses assume a high degree of symmetry, which makes unclear the extent to which the results will apply in more realistic models of collapse, they do provide another indication that fragmentation in real protogalaxies will be far less effective than the hierarchical fragmentation scenario assumes.

3.5. OTHER FORMS OF FRAGMENTATION

In view of the doubts raised in the previous section concerning the effectiveness of fragmentation driven purely by gravity, it is worthwhile to spend some time examining two other processes which may bring about fragmentation of the protogalactic gas: thermal instability and supersonic turbulence.

3.5.1. *Thermal instability*

So far we have considered the gas pressure purely as a stabilizing force, resisting the action of gravity. However, if the protogalactic gas is thermally unstable, then the pressure can itself drive fragmentation within the gas.

Thermal instability occurs when small perturbations to the density and/or temperature of a region of gas cause the subsequent temperature evolution of that region to differ significantly from that of the unperturbed gas. The case of interest to us is the one in which the perturbations cause accelerated cooling of the perturbed region. This was first investigated by Parker (1953), who derived an instability criterion

$$\left(\frac{\partial \mathcal{L}}{\partial T}\right)_\rho < 0, \quad (34)$$

where $\mathcal{L} = (\Lambda - \Gamma)/\rho$ is the specific heat loss function, under the assumption that the perturbations were isochoric (i.e. that the gas maintained

a constant density). Field (1965) pointed out that in this case, pressure gradients would develop in the gas, and that thermal instability could therefore drive dynamical flows. He also argued that on small scales, the gas would rapidly respond to any change in temperature by changing its density, so as to keep its pressure constant. In other words, small perturbations would evolve isobarically rather than isochorically. Field (1965) derived an instability criterion for the isobaric case

$$\left(\frac{\partial\mathcal{L}}{\partial T}\right)_p = \left(\frac{\partial\mathcal{L}}{\partial T}\right)_\rho - \frac{\rho_0}{T_0} \left(\frac{\partial\mathcal{L}}{\partial\rho}\right)_T < 0, \quad (35)$$

where ρ_0 and T_0 are the unperturbed density and temperature. This is the correct criterion for perturbations with wavelengths $\lambda_F < \lambda < \lambda_c$, where $\lambda_c = c_s t_{\text{cool}}$ is the distance travelled by a sound wave in a single cooling time in the unperturbed medium, and where λ_F is the Field length, given by

$$\lambda_F = \left(\frac{\kappa T}{\Lambda}\right)^{1/2}, \quad (36)$$

where κ is the coefficient of thermal conduction. For perturbations with $\lambda > \lambda_c$, Parker's isochoric criterion applies, while for perturbations with $\lambda < \lambda_F$, thermal conduction completely suppresses the instability.

If we apply these criteria to primordial gas, while keeping the chemical composition of the gas fixed, then we find that the gas is always thermally stable. However, if we allow the chemical composition of the gas to vary as we perturb the temperature and density, then various *chemo-thermal* instabilities become possible. The simplest of these occurs in very hot gas with $10^5 < T < 10^7$ K. Within this temperature regime, cooling via He II line emission increases sharply with decreasing temperature as helium recombines from He III to He II, leading to a pronounced thermal instability. This instability has been investigated in the context of galaxy formation by Murray and Lin (1990, 1996; see also Lin and Murray, 1992, 2000) but seems unlikely to play a significant role in the evolution of the first protogalaxies, as the protogalactic gas never becomes hot enough to trigger it.

At lower temperatures, various instabilities associated with the formation and dissociation of H_2 may occur. The first of these was identified by Sabano and Yoshii (1977) and analyzed in more detail by Yoshii and Sabano (1979). It occurs in gas with a temperature in the range $2000 \lesssim T \lesssim 4000$ K (with a slight dependence on density) and is caused by the collisional dissociation of H_2 . Within this temperature range, the equilibrium abundance of H_2 is a sensitive function of temperature, due to the strong temperature dependence of the collisional dissociation rate (reaction R9). Therefore, gas which has a slightly lower temperature than its surroundings will have a higher H_2 abundance, and hence

a higher cooling rate. If this leads to a further drop in temperature and increase in H_2 abundance, then an instability results. Gas cooler than about 2000K does not suffer from the instability because the collisional dissociation rate becomes too small to significantly affect the H_2 abundance, which therefore loses its strong temperature dependence, while in gas hotter than about 4000 K, the H_2 abundance becomes too small to provide effective cooling.

Silk (1983) identified a related instability that appears once the three-body formation of H_2 becomes effective and occurs for a similar reason: a small decrease in the temperature and the associated increase in the density lead to an enhanced H_2 abundance and higher cooling rate, which further perturb the temperature. This instability vanishes if the gas becomes fully molecular or becomes optically thick to H_2 line emission.

Finally, another potential instability has recently been identified by Ripamonti and Abel (2004). This one occurs at very high densities ($10^{14} < n < 10^{15} \text{ cm}^{-3}$) and is due to a combination of the onset of collisionally-induced emission from the H_2 (which is highly sensitive to the gas density and which quickly comes to dominate the H_2 cooling rate), and a renewed phase of collisional dissociation within the dense gas (which at slightly lower densities is fully molecular). However, the resulting instability is very sensitive to the temperature of the gas, as can be seen clearly from figures 7 and 8 of Ripamonti and Abel (2004), and it remains to be seen whether this instability will actually occur in practice.

Since thermal instability is capable of creating dense structure in the gas on all scales larger than the Field length, we might expect it to profoundly influence the ability of the gas to fragment. However, in practice, it is unlikely to be of great importance in primordial gas. There are two main reasons for this. First, the H_2 -related instabilities discussed above all operate within a fairly restricted range of temperatures. This significantly limits the size of the temperature contrasts that can be created, which in turn limits the size of the resulting density contrasts, which can therefore be disrupted more easily by other processes such as turbulence (Abel, Bryan, and Norman, 2002). Second, thermal instabilities grow on the cooling timescale, t_{cool} , and will therefore cause significant restructuring of the gas only when $t_{\text{cool}} \ll t_{\text{dyn}}$. However, Omukai and Yoshii (2003) and Ripamonti and Abel (2004) demonstrate that thermally unstable protogalactic gas typically has $t_{\text{cool}} \simeq t_{\text{dyn}}$, implying that the instabilities do not have sufficient time to grow. This conclusion is supported by the results of Abel, Bryan, and Norman (2002), whose simulation includes gas in the thermally unstable regime

associated with three-body H_2 formation, but who find no indication that this instability has any significant dynamical effect.

3.5.2. *Supersonic turbulence*

Another way to create dense structures in the gas without the assistance of gravity is by compressing it in shocks. In particular, if the velocity field of the gas is turbulent and supersonic, then large density enhancements can be created as the gas is repeatedly shocked. This is a process that has received considerable attention in a Galactic context, since there is substantial observational evidence for the existence of supersonic turbulence in interstellar gas on all scales larger than a few tenths of a parsec. Rather than attempting to summarize all of this material here – a hopeless task – I refer the reader to the recent comprehensive reviews of Mac Low and Klessen (2004), Elmegreen and Scalo (2004) and Scalo and Elmegreen (2004), and restrict my discussion to a few points of particular relevance to primordial star formation.

Simulations of supersonic turbulence in self-gravitating, isothermal gas have been performed by a number of groups (Ostriker, Gammie, and Stone, 1999; Klessen, Heitsch, and Mac Low, 2000; Heitsch, Mac Low, and Klessen, 2001; Gammie *et al.*, 2003; Bate, Bonnell, and Bromm, 2003; Li *et al.*, 2004). The gas in these simulations rapidly develops a highly inhomogeneous structure, with a density probability distribution function (PDF) which is approximately log-normal. Dense, gravitationally bound cores form in the highest density regions, with a mass spectrum that also appears to be log-normal and which resembles the stellar IMF. The efficiency with which cores form depends upon the properties of the turbulence, and is lower in models with more power on smaller spatial scales (Klessen, Heitsch, and Mac Low, 2000), but it appears to be very difficult to completely suppress fragmentation: this would require strong turbulence on very small scales, which would rapidly decay away (Stone, Ostriker, and Gammie, 1998; Mac Low, 1999) unless driven by some form of energy input on those scales.

A series of attempts have been made to relate the stellar IMF directly to the statistical properties of interstellar turbulence (Larson, 1981; Fleck, 1982; Elmegreen, 1993; Padoan, 1995; Padoan, Nordlund, and Jones, 1997; Myers, 2000; Padoan and Nordlund, 2002), which would allow the IMF to be predicted in environments such as early protogalaxies for which no direct observational determinations exist. However, none of these attempts have met with widespread acceptance, and research in this area is still ongoing.

Extension of these results to primordial gas is further complicated by the fact that most studies of turbulent fragmentation assume an

isothermal equation of state. This is a reasonable approximation for gas in local molecular clouds, since its cooling time is very short, but it is unlikely to be appropriate for primordial gas with $t_{\text{cool}} \sim t_{\text{dyn}}$. Since there are indications that relatively small changes in the equation of state can have a large effect on both the shape of the density PDF (Passot and Vázquez-Semadeni, 1998) and on the numbers and masses of self-gravitating cores that form (Li, Klessen, and Mac Low, 2003), a straightforward extrapolation from the isothermal results appears unwise. Work in this area is ongoing.

3.6. NUMERICAL SIMULATIONS

As the previous sections hopefully make clear, a number of different factors influence the ability of the protogalactic gas to fragment. While we can gain considerable insight into the physics of the individual processes through the use of simple analytical models, for a proper understanding of how the various different processes interact within a real protogalaxy we are currently forced to turn to numerical simulations.

3.6.1. *Simulations of local star formation*

Before discussing the results of simulations designed specifically to study protogalactic fragmentation and primordial star formation, it seems worthwhile to examine what we can learn from simulations designed primarily to study local star formation.

One important thing that we have learnt from this kind of simulation is the vital importance, when studying gravitational collapse and fragmentation, of resolving the Jeans length throughout the simulation. This was convincingly demonstrated by Truelove *et al.* (1997), who showed that if this criterion is not met, then completely artificial fragmentation of the gas can result. This implies that simulations that fail to meet this criterion cannot be used to make meaningful predictions about gravitationally-driven fragmentation. Although Truelove *et al.* (1997) restricted their attention to grid-based simulations, it has been shown that SPH simulations suffer from a very similar problem (Bate and Burkert, 1997; Whitworth, 1998).

Also of interest are the results of a set of simulations performed by Tsuribe and Inutsuka (1999ab). They used high resolution SPH simulations to study the isothermal collapse of a set of uniform spherical clouds with varying ratios of thermal to gravitational energy, parameterized by

$$\alpha_0 = \frac{5c_s^2 R_0}{2GM}, \quad (37)$$

where R_0 is the initial radius of the cloud, and of rotational to gravitational energy, parameterized by

$$\beta_0 = \frac{\Omega_0^2 R_0^3}{3GM}, \quad (38)$$

where Ω_0 is the initial angular velocity. Previous analytical and numerical work (Tohline, 1981; Miyama, Hayashi, and Narita, 1984) suggested that such a cloud would collapse to a disk, with a flatness that depended on the product $\alpha_0\beta_0$, and that for $\alpha_0\beta_0 < 0.12$, this disk would subsequently fragment. However, this criterion is clearly not correct when β_0 is very small, as it predicts that a cloud with $\alpha_0 > 1$ should collapse and fragment, whereas in reality such a cloud would have a mass smaller than the Jeans mass, and would not collapse. Moreover, the analytical derivation of this criterion assumes that the collapse is homologous, while in reality collapsing clouds would tend to become centrally concentrated.

Tsuribe and Inutsuka find three possible outcomes for their simulated clouds. When α_0 and β_0 are both small, the cloud collapses to a thin disk and fragments, much as was previously envisaged. As α_0 increases, however, the thickness of the disk also increases, and once its flatness – defined simply as the ratio of its radius to its scale height – falls below a value of approximately 4π , the disk no longer fragments. Further increases in α_0 lead to a final state that increasingly comes to resemble the so-called Larson-Penston similarity solution.⁴ Finally, for sufficiently large α_0 , collapse is entirely suppressed.

In the low β_0 limit, the boundary between fragmentation and self-similar collapse occurs for $\alpha_0 \simeq 0.5$; with increasing β_0 , the boundary moves to smaller α_0 , and is given approximately by $\alpha_0 = 0.55 - \beta_0$ for $0 < \beta_0 < 0.3$.

Although the initial conditions for these simulations are highly idealized, they do provide strong support for some of the criticisms of the hierarchical fragmentation scenario discussed in section 3.1, and demonstrate that gravitational fragmentation does not appear to be

⁴ The Larson-Penston solution is an asymptotic similarity solution for the isothermal collapse of a sphere, independently derived by Larson (1969) and Penston (1969), which describes the collapse at late times and/or at small distances from the centre, when the influence of the boundary conditions has become negligible. It can be derived numerically from the governing equations of the flow if one assumes that the flow is smooth (i.e. that there are no shocks) and that the central velocity is zero; this derivation can also be generalized to the case of a polytropic equation of state $P = K\rho^\gamma$ (Larson, 1969). Although other similarity solutions are possible (Shu, 1977; Hunter, 1977; Whitworth and Summers, 1985), the Larson-Penston solution appears to provide the best fit to the results of numerical simulations of isothermal spherical collapse (Foster and Chevalier, 1993).

as effective as originally anticipated, particularly in clouds with large values of α_0 .

Tsuribe and Inutsuka (2001) extended this analysis, in a more limited fashion, to the case of protogalactic collapse. They performed three large SPH simulations of the collapse of uniform, spherical protogalaxies, all with the same initial temperature ($T_0 = 150$ K) and rotation parameter ($\beta_0 = 0.25$), but with differing masses: $M = 10^6, 3 \times 10^6, 10^7 M_\odot$, implying that $\alpha_0 = 0.18, 0.09$ and 0.04 respectively. Rather than assuming that the gas remains isothermal, Tsuribe and Inutsuka follow its chemical and thermal evolution during the collapse. Based on the previous isothermal results, one would expect fragmentation to occur in all three simulations, but in fact fragmentation does not occur in the $10^6 M_\odot$ protogalaxy, which instead simply forms a single dense central core. This difference from the isothermal case is presumably due to the fact that cooling is less efficient in these more realistic model protogalaxies, which therefore evolve as if they had larger values of α_0 . If this interpretation is correct, then it suggests that we can treat Tsuribe and Inutsuka's isothermal fragmentation criterion as a necessary, but not sufficient, criterion for fragmentation within primordial gas. As we shall see below, this interpretation is consistent with the results of more detailed protogalactic simulations.

3.6.2. *Filamentary collapse*

The propensity of gravitationally collapsing spheres of gas to settle into disks even when β_0 is small, noted by Tsuribe and Inutsuka and by many other authors, is not unexpected, since we have known for a long time that small departures from spherical symmetry are steadily magnified during free-fall collapse (Lin, Mestel, and Shu, 1965). Moreover, flattened, disk-like clouds will generally fragment into filamentary structures (Miyama, Narita, and Hayashi 1987ab) which only subsequently fragment into clumps. In light of this, a number of authors have considered the problem of filamentary collapse in primordial gas.

A pressure-supported filament (i.e. one which is not collapsing or expanding radially) is gravitationally unstable to perturbations along the axis of the filament. Moreover, it is possible to show that for an isothermal filament, the fastest growing perturbation is the one with wavelength $\lambda_c \sim \pi R$, where R is the scale radius of the filament, defined as:

$$R = \left(\frac{M}{\pi \rho_0} \right)^{1/2}, \quad (39)$$

and where M is the mass per unit length and ρ_0 is the central density (Stodólkiewicz, 1963). A similar result can be derived for a polytropic filament (Larson, 1985). However, filaments formed during protogalac-

tic collapse are unlikely to start in hydrostatic equilibrium in the radial direction. Uehara *et al.* (1996) argue that in that case, it is necessary to follow the radial evolution of the filament until such time as the contraction timescale, given by $t_{\text{con}} = \rho_0/\dot{\rho}_0$, exceeds the fragmentation timescale, $t_{\text{frag}} \sim (G\rho_0)^{-1/2}$; at this point, the equilibrium analysis can be applied to give an estimate of the resulting fragment mass.

Uehara *et al.* (1996) used this approach to study the fragmentation of primordial filaments with a range of values of M . They adopted an initial temperature, density and molecular fraction appropriate to gas that had already undergone significant cooling and collapse within a protogalaxy, consistent with their assumption that the filaments had formed in a fragmenting disk. They followed the subsequent chemical and thermal evolution of the filament in some detail, but treated the density evolution in an approximate fashion: the scale radius was assumed to evolve as

$$\ddot{R} = -\frac{2G}{R} [M - M_c(T)], \quad (40)$$

where M_c is the mass per unit length of an equilibrium isothermal cylinder (Ostriker, 1964)

$$M_c(T) = \frac{2kT}{\mu m_{\text{H}}G}, \quad (41)$$

in which case the density then follows from Equation (39). They studied a number of different collapses, with values of M ranging from $1-2 M_c$. They found that as M increased, there was a corresponding increase in the density at which the filament fragmented, and a consequent decrease in the fragment mass M_F , which fell from $100 M_{\odot}$ for $M = M_c$ down to $2 M_{\odot}$ for $M = 2M_c$.

Nakamura and Umemura (1999) reconsidered this problem and improved on the Uehara *et al.* (1996) analysis in several important respects. Most significantly, they replaced the approximate treatment of the density evolution used by Uehara *et al.* with a more accurate treatment based on a one-dimensional hydrodynamic simulation of the collapse of the filament. They also made use of a more extensive chemical model and considered a wider range of initial conditions. They found that the collapse led to one of two possible outcomes, depending on the initial temperature and the value of $f \equiv M_c/M$. In the majority of the models, H_2 cooling was effective at the start of the simulation and remained so until the gas became optically thick at high density ($n \sim 10^{11} \text{ cm}^{-3}$). This allowed the filaments to collapse dynamically to high density, fragmenting only once cooling became ineffective, and producing fragments with masses $M_F \sim 1-10 M_{\odot}$. However, in models

where the initial temperature was low ($T_0 = 100$ K), H_2 cooling was not immediately effective, and the initial evolution of the filament was adiabatic. In models where the mass per unit length was large ($f > 2$), collapse could persist until the temperature increased to a point at which H_2 cooling became effective, following which the evolution of the filament would continue much as if it had started with a higher initial temperature. If the initial mass per unit length were small, however, then collapse would very quickly come to an end, resulting in an equilibrium filament with a relatively low central density ($n \sim 10^5 \text{ cm}^{-3}$) that would produce much larger fragments with masses of a few hundred M_\odot .

Nakamura and Umemura (2001) further improved the treatment of this problem by performing two-dimensional axisymmetric hydrodynamical simulations of filamentary collapse, which allowed them to follow the fragmentation numerically, rather than estimating its effects analytically. They again examined a wide range of initial conditions, although in light of their previous results, they restricted their attention to filaments with initial temperatures $T_0 \geq 300$ K. Once more, they found two possible outcomes. In filaments with a low initial density ($n \lesssim 10^5 \text{ cm}^{-3}$), fragmentation occurred prior to the onset of three-body H_2 formation and the resulting fragments were large, with masses $M_F \sim 100 M_\odot$. On the other hand, in filaments with a high initial density, fragmentation is delayed until after the gas has become optically thick, resulting in much smaller fragments of mass $M_F \sim 1\text{--}2 M_\odot$.

The potential role played by HD molecules in filamentary collapse has been investigated by Uehara and Inutsuka (2000) and Nakamura and Umemura (2002). Uehara and Inutsuka assumed that the filaments formed in a shock-bounded sheet, and therefore adopted initial conditions appropriate to primordial gas which has cooled rapidly from temperatures $T \gg 10^4$ K. As previously demonstrated by Mac Low and Shull (1986) and Shapiro and Kang (1987), hydrogen recombination lags behind cooling in such gas, resulting in an elevated fractional ionization that allows a substantial H_2 fraction ($f_{\text{H}_2} \sim 10^{-2}$) to build up. Uehara and Inutsuka demonstrate that in these conditions, the fractional abundance of HD would be of order 10^{-5} , and showed that this amount of HD is enough to cool the filament to 50 K and to keep it evolving isothermally at this temperature until the HD lines become optically thick. They argued that this allows very low mass fragments to form, with masses $M_F \sim 0.01\text{--}0.1 M_\odot$.

Nakamura and Umemura (2002) examined collapse from a wider range of initial conditions than Uehara and Inutsuka (2000), and showed that HD cooling would only be significant if the initial H_2 and HD abundances were both large. However, even in this case, they obtained

a much larger fragment mass than Uehara and Inutsuka (2000), finding $M_F \sim 10M_\odot$. They ascribe this difference in part to their more detailed treatment of optical depth effects, and in part to the fact that Uehara and Inutsuka assumed that the minimum fragment mass would equal the Jeans mass, rather than the mass contained within the fastest growing perturbation, which in this case is about an order of magnitude larger.

Filamentary collapse has also been studied by Flower (2002) and Flower and Pineau des Forêts (2003), who examined the effects of including a magnetic field. Flower (2002) used a dynamical treatment similar to that of Uehara *et al.* (1996) to show that even a relatively weak axial magnetic field would soon provide enough pressure to halt the collapse, resulting in the formation of massive fragments, with sizes ranging from $M_F \sim 60 M_\odot$ for an initial field strength of 10^{-9} G up to $M_F \sim 6000 M_\odot$ for an initial field strength of 10^{-7} G. However, Flower and Pineau des Forêts (2003) subsequently showed that if the effects of ambipolar diffusion were also included, then the field would be far less effective at slowing the collapse, since the fractional ionization of the gas in the filament is too low to keep the field strongly tied to the gas.

Ultimately, in spite of the attention paid to filamentary collapse, the relevance of these results to fragmentation in real protogalaxies remains unclear. The main concerns are that all of these simulations assume initial conditions that are far more smooth and symmetrical than will actually be the case in a real collapse, and that they neglect a number of potentially important effects such as rotation and turbulence.

3.6.3. *Three-dimensional simulations of protogalactic collapse*

Relatively few 3D simulations of protogalaxy formation have been performed to date, and of these the only ones with sufficient dynamical range to study fragmentation within the newly formed protogalaxy are the SPH simulations of Bromm, Coppi, and Larson (1999, 2002), and the adaptive mesh refinement simulations of Abel, Bryan, and Norman (2000, 2002), both of which were discussed previously in section 2.5.

As previously noted, Bromm, Coppi, and Larson study collapse from somewhat idealized initial conditions: a single, isolated overdensity, in rigid rotation with spin parameter λ , and set to collapse at some specified redshift z_c . They begin their simulations at $z = 100$, and evolve from then until shortly after the protogalaxy has virialized. By focusing on a single protogalaxy in this way they are able to achieve a high mass resolution. The precise resolution depends on the mass of the protogalaxy simulated and the number of SPH particles used, but for their fiducial case of a $2 \times 10^6 M_\odot$ protogalaxy with a baryon

fraction of 5%, simulated with 16384 particles, Bromm, Coppi, and Larson achieve a mass resolution of approximately $200 M_{\odot}$. To avoid the numerical difficulties that would otherwise force the simulations to be halted once the Jeans mass fell below this value (Bate and Burkert, 1997; Whitworth, 1998), Bromm, Coppi, and Larson make use of a sink particle technique (Bate, Bonnell, and Price, 1995). SPH particles with densities greater than a threshold value $n_{\text{th}} = 10^8 \text{ cm}^{-3}$ and which are in regions of converging flow ($\nabla \cdot \mathbf{v} < 0$) are removed from the simulation, and replaced with one or more sink particles. One sink particle is created for each individual collapsing region, with a mass and momentum equal to the sum of the masses and momenta of the particles that it has replaced. Once created, sink particles continue to interact with the surrounding gas particles, and can accrete them if they lie within two smoothing lengths and satisfy the criteria above. Further details of the algorithm are given in Bromm, Coppi, and Larson (2002).

Bromm, Coppi, and Larson (1999) present results from a single simulation of protogalactic collapse. The protogalaxy they simulate has a total mass of $2 \times 10^6 M_{\odot}$, a baryon fraction of 5%, a spin parameter $\lambda = 0.05$, and collapses at a redshift $z = 30$. Following the initial sequence of compression, shock and subsequent cooling and settling that has already been described in section 2.5, Bromm, Coppi, and Larson find that the cooled gas settles into a flattened central disk, with a radius of approximately 15 pc and thickness of 2 pc. This disk rapidly breaks up into about a dozen dense clumps, with masses ranging from $200\text{--}10^4 M_{\odot}$. The gas in the disk has a mean temperature of approximately 200 K (although there is considerable scatter about this value), and a density of order 10^4 cm^{-3} . The gas in the clumps is somewhat hotter ($T \sim 500 \text{ K}$) and substantially denser, with densities ranging all the way up to n_{th} . Bromm, Coppi, and Larson (1999) find no evidence for further fragmentation of the clumps, but since they are soon replaced in the simulation by sink particles, they are unable to rule it out. However, further fragmentation of the clumps appears unlikely: they have relatively large ratios of thermal to gravitational energy ($\alpha_0 \simeq 0.5$ for a typical clump), and so based on the Tsuribe and Inutsuka criterion, one would not expect them to fragment.

Bromm, Coppi, and Larson (2002) discuss the results of a more extensive range of simulations, which sample a wider range of initial conditions. They find that the thermodynamic behaviour of the gas is very similar in each of their simulations. In every case, the gas cools rapidly until it reaches a temperature and density at which cooling becomes ineffective. In a gas dominated by H_2 cooling, this occurs at $T \sim 200 \text{ K}$ and $n \simeq 10^4 \text{ cm}^{-3}$: below this temperature, the H_2

cooling rate falls off exponentially, while above this density, collisional de-excitation of the excited levels of H_2 significantly reduces its effectiveness as a coolant. Since fragmentation typically occurs after the gas has reached this state, the fragment masses tend to lie close to the Jeans mass corresponding to this temperature and density.

In contrast, the morphology of the cool gas is far more sensitive to the initial conditions of the simulation. In most cases, it is disk-like, but the size and visual appearance of the disks alter significantly as the spin parameter and the collapse redshift are varied. A notable exception is the single low-mass protogalaxy simulated by Bromm, Coppi, and Larson (2002), which had a total mass $M = 2 \times 10^5 M_\odot$, and the usual baryonic fraction of 5%. This had a larger degree of pressure support than the more massive protogalaxies, and settled into a spheroidal, quasi-hydrostatic equilibrium configuration at a density of order 10^2 cm^{-3} . Bromm, Coppi, and Larson found no evidence for fragmentation within this protogalaxy, although a single massive dense clump did form in its centre, much as in the high α_0 simulations of Tsuribe and Inutsuka (1999a).

Finally, Bromm, Coppi, and Larson also examined the effects of HD cooling and showed that it made very little difference to the outcome of the simulation. This appears to be due to the fact that although HD becomes the dominant coolant in low temperature gas, it never becomes an *effective* coolant – the cooling time of the gas remains significantly longer than the dynamical time, and so the gas does not become significantly cooler than it would if the HD were not included in the simulation.

Abel, Bryan, and Norman (2000, 2002) pursued a rather different strategy in their study of protogalactic collapse. Rather than simulating collapse from a range of different initial conditions, they instead focused on simulating a single example in great detail, starting from realistic initial conditions within a large simulation volume, and following the collapse to higher densities than those reached in Bromm, Coppi, and Larson’s SPH simulations. On large scales, their results agree with those of other simulations of protogalactic collapse, as I have already discussed in section 2.5. On smaller scales, they find an accumulation of cold gas within the central ten parsecs of the protogalaxy, much as Bromm, Coppi, and Larson do. However, the morphology of this gas is not at all disk-like – it is more like a slightly flattened spheroid, although less symmetric than this description suggests. Abel, Bryan, and Norman find no evidence for any fragmentation of this cool gas, beyond the formation of a single dense core of mass $M \sim 100 M_\odot$ at its centre.

At the moment that it forms, this central core has a similar temperature and density to the surrounding cool gas, namely $T \simeq 200$ K and $n \simeq 10^4$ cm $^{-3}$, giving it a ratio of thermal to gravitational energy $\alpha_0 \simeq 0.5$. It is also rotating slowly, with $\beta_0 = 0.01$. These values suggest that even if the core were to collapse isothermally, it would be unlikely to fragment further. In fact, the collapse of the core is not isothermal: instead, the gas rapidly heats up to a temperature of about 800K. Indeed, it is this sharp rise in temperature, as much as anything, that distinguishes the core from its surroundings, as its density profile merges smoothly with the surrounding gas.

This rise in temperature, which is also seen in the cores that form in the Bromm, Coppi, and Larson simulations, albeit to a lesser degree, is a natural consequence of the reduced efficiency of H $_2$ cooling at high densities. Above a critical density of approximately 10^4 cm $^{-3}$, the H $_2$ cooling rate begins to scale as $\Lambda_{\text{H}_2} \propto n$, while the compressional heating rate scales as $\Gamma_{\text{comp}} \propto n^{3/2}$, and so the latter eventually begins to dominate, causing the core temperature to increase.

In their original simulation, Abel, Bryan, and Norman followed the evolution of the core only up to a density of 10^8 cm $^{-3}$; as their chemical model did not include 3-body H $_2$ formation, which becomes effective at this density, any results from higher densities would have been highly inaccurate. In their subsequent simulation, they included the three body reactions, allowing them to follow the collapse of the core to much higher densities. They were eventually forced to stop at a density of 10^{13} cm $^{-3}$, because the H $_2$ rotational and vibrational lines were becoming optically thick, and their assumption of optically thin cooling was therefore no longer valid.

Abel, Bryan, and Norman found no evidence for fragmentation of the central core in either of their simulations. In particular, the thermal instability associated with H $_2$ formation and discussed in section 3.5.1 appears to have only a minor effect on the evolution of the core, and does not cause it to fragment. Turbulence is also ineffective at driving fragmentation, since the collapse is predominantly subsonic, only becoming marginally supersonic within the central 10–20 AU near the end of the simulation.

Finally, Abel, Bryan, and Norman show that the core never becomes rotationally supported, and that its final rotational velocity is about half of the Keplerian orbital velocity $v_{\text{Kep}} = (GM/r)^{1/2}$. This is one of their most surprising results, as it implies that angular momentum is being transferred outwards during the evolution of the core. Indeed, Abel, Bryan, and Norman are able to demonstrate directly that this is occurring (see figure 4a of Abel, Bryan, and Norman, 2002). This result inevitably raises the suspicion that it is due to some purely numerical

effect, such as numerical shear viscosity (Norman, Wilson, and Barton, 1980). However, Abel, Bryan, and Norman find that the details of the angular momentum transfer are independent of the hydrodynamic algorithm used and of the spatial resolution (provided that the simulation continues to satisfy the Truelove criterion). This suggests that the effect that they find is real, but of course is not yet conclusive; it would be extremely useful to be able to reproduce this result with another hydrodynamical code, ideally one based on a fundamentally different algorithm, such as SPH.

Abel, Bryan, and Norman (2002) ascribe the angular momentum transfer to the action of shocks during the collapse, but this conclusion is open to question since, as noted above, the infall is subsonic in most of the core. Another possibility is that angular momentum is transferred by tidal interactions with external mass concentrations (Larson, 2002). Ultimately, to develop an understanding of the physics underlying this effect, we are likely to require additional high resolution adaptive mesh simulations (Norman, 2003).

3.6.4. *The optically thick phase*

To follow the evolution of the gas beyond the density reached by Abel, Bryan, and Norman (2002), it is necessary to solve a radiative transfer problem for the optically thick H_2 line emission, in order to be able to calculate the correct cooling rate. Unfortunately, an exact solution of this problem within a three-dimensional hydrodynamical simulation is not currently feasible, since it is essentially a seven-dimensional problem (three spatial dimensions, two angles plus frequency and time). Approximate methods, such as the OTVET formalism of Gnedin and Abel (2001) will help in the near future, but so far the only simulations that have been performed of this last stage of protogalactic evolution have been forced to assume spherical symmetry, purely for reasons of efficiency. This unfortunately renders them mute on such topics of interest as whether the efficient outward transfer of angular momentum found by Abel, Bryan, and Norman continues at higher densities, or whether the core fragments into a close binary or multiple system rather than a single star.

The first detailed simulations of the evolution of the core in the optically thick phase were performed by Omukai and Nishi (1998). They used an explicit one-dimensional Lagrangian hydrodynamical code to simulate the collapse of a small number of model cores with different masses and densities. At gas densities below 10^{15} cm^{-3} , they followed the chemical evolution of the gas using a simplified chemical model based on that of Palla, Salpeter, and Stahler (1983); at higher densities, chemical equilibrium was assumed, and the chemical abundances were

obtained from solution of the coupled Saha equations. Cooling from both H₂ line emission and collision-induced continuum emission was included; the latter dominates at very high densities. Omukai and Nishi computed the radiative transfer of this emission using the tangent ray method (Hummer and Rybicki, 1971), under the assumption that line transfer and continuum transfer can be decoupled. To further simplify the calculation, they assumed that the diffusion approximation holds in regions that are highly opaque in the continuum, and that line cooling from this gas was negligible.

Omukai and Nishi found that after a short initial transient, the evolution of each of their model cores was essentially the same, and so they presented detailed results for only a single example: a polytropic core of mass $M = 100 M_{\odot}$ and density at the half-mass radius $n_{\text{h}} = 10^6 \text{ cm}^{-3}$. As it collapsed, this core quickly developed a self-similar density profile with $\rho \propto r^{-2.2}$, and the collapse as a whole was well described by a Larson-Penston type similarity solution for a gas with an equation of state $p = K\rho^{\gamma}$, where $K = 4.2 \times 10^{11}$ (in cgs units), and $\gamma = 1.09$. The gas in the centre of the collapsing core soon became optically thick in the H₂ lines, but this did not immediately lead to the evolution becoming adiabatic, as enough cooling was possible through the optically thin wings of the lines, as well as in the continuum via collision-induced emission, to maintain $\gamma_{\text{eff}} < 4/3$ for an extended period. Eventually, however, the core temperature became high enough to thoroughly dissociate H₂, and the evolution became fully adiabatic. This occurred for a central density $n_{\text{c}} = 10^{22} \text{ cm}^{-3}$, and led to the formation of a small hydrostatic core, with mass $M = 5 \times 10^{-3} M_{\odot}$, at the centre of the flow. This core rapidly became fully ionized, and was bounded by an accretion shock at a radius of 2 AU, and it seems natural to identify it as a protostar. Unfortunately, Omukai and Nishi were unable to follow its subsequent evolution, as the Courant timestep became prohibitively small once the core had formed, forcing them to terminate their simulation.

More recently, Ripamonti *et al.* (2002) also simulated the optically thick collapse phase. Their basic approach was similar to that of Omukai and Nishi (1998), but with two major improvements: they included a term in the momentum equations corresponding to the force exerted on the gas by the scattered H₂ emission, and they used a more detailed model for the chemical evolution of the gas and the behaviour of the equation of state at very high densities, based on Saumon, Chabrier, and van Horn (1995). In addition, they also examined a wider range of initial conditions. Despite this, they found essentially the same behaviour as Omukai and Nishi. The evolution of the model cores was strongly convergent and soon became well described by a

Larson-Penston type similarity solution. This self-similarity lasted until a small hydrostatic core of mass $3 \times 10^{-3} M_{\odot}$ formed at the centre of the flow.

3.7. SUMMARY

In the introduction, I posed a number of questions concerning the evolution of gas within newly formed protogalaxies, namely: does the gas fragment? If so, how large are the fragments? And when and why does fragmentation stop?

Much of the work that has been done on primordial star formation assumes some version of the hierarchical fragmentation scenario, in which fragmentation is highly efficient and is terminated only by the transition of the gas from isothermal to adiabatic evolution. In these models, the main uncertainties are the cause of this transition – chemical changes or fragment opacity? – and the temperature and density at which it occurs.

However, as I outlined in section 3.4, there are a number of reasons to believe that hierarchical fragmentation does not occur in real protogalaxies as various effects combine to inhibit fragmentation. This conclusion is supported by the results of the simulations of Tsuribe and Inutsuka (1999ab, 2001), Bromm, Coppi, and Larson (1999, 2002) and Abel, Bryan, and Norman (2000, 2002): in each of these simulations there is at most a single episode of fragmentation, and no evidence for any subfragmentation (i.e. fragmentation of the fragments). Moreover, in some of these simulations, such as Abel, Bryan, and Norman (2000, 2002), the use of the word ‘fragmentation’ to describe the evolution of the gas is misleading: the single ‘fragment’ that forms is actually just the central dense core of a more extended density distribution.

Why is it that fragmentation is so inefficient? Inefficient fragmentation appears to be a natural outcome of quasi-spherical collapse in gas with a high ratio of thermal to gravitational energy. During such a collapse, the large thermal pressure will create a strongly peaked density distribution, even if the gas is initially quite uniform. It will also suppress small-scale collapse until the density of the gas has increased by a large factor, since the local Jeans mass scales as $M_J \propto n^{-1/2}$ in isothermal collapse. In combination, these effects imply that the gas at the centre of the protogalaxy will quickly come to have both the smallest Jeans mass and the shortest free-fall time and therefore, unless its collapse is delayed or halted in some way, it will continue to collapse all the way to protostellar densities before the bulk of the gas has had the opportunity to fragment. If this interpretation is correct,

it suggests that further fragmentation may occur within, say, the Abel, Bryan, and Norman simulations, if they were continued past the point at which the first star forms. However, since this first star will exert a strong feedback on its surroundings on a short timescale (Omukai and Nishi, 1999; Glover and Brand, 2001; Bromm, Yoshida, and Hernquist, 2003; Whalen, Abel, and Norman, 2003) it appears unlikely that any further fragmentation would in fact occur.

The efficacy of fragmentation could be enhanced by delaying the collapse of the densest gas, giving the lower density gas more time in which to fragment. As Bromm, Coppi, and Larson demonstrate, rotation can do this to some extent, but the outward transfer of angular momentum identified by Abel, Bryan, and Norman makes it less effective than simple estimates would suggest. Strong perturbations arising from thermal instability or supersonic turbulence could also boost fragmentation, but in practice neither process is particularly effective in primordial gas.

The few fragments which do form typically have initial masses of a few hundred M_{\odot} . This particular mass scale appears to be a consequence of the thermodynamics of the gas. At densities less than the H_2 critical density of 10^4 cm^{-3} , H_2 cooling is efficient, and the gas can cool to a minimum temperature of about 200 K. At higher densities, H_2 cooling becomes less efficient, and the gas heats up. These values of density and temperature therefore mark the point at which isothermal evolution comes to an end and γ_{eff} first exceeds one, and so it is not surprising that the minimum fragment mass corresponds approximately to the value of the Jeans mass at this density and temperature.

The major uncertainty that remains concerns the behaviour of the collapsing gas in the optically thick regime. It may continue to collapse quasi-spherically, in which case we would expect a single, low-mass protostellar core to eventually form, as in the simulations of Omukai and Nishi (1998) and Ripamonti *et al.* (2002). On the other hand, it may form a gravitationally unstable disk, in which case fragmentation into a binary or multiple system would appear to be more likely. Resolution of this uncertainty awaits the development of an accurate and efficient way of treating the thermal evolution of the optically thick gas.

4. Protostellar accretion and the final stellar mass

The results of the simulations of Omukai and Nishi (1998) and Ripamonti *et al.* (2002) suggest that the initial mass of a primordial protostar may be very small, no more than a few thousandths of a solar mass. However, this small initial protostar will be surrounded by

a large envelope of infalling gas, some fraction of which will inevitably be accreted by the protostar.

If mass loss from the protostar is negligible (which seems to be a good approximation even for very massive metal-free stars – see Marigo, Chiosi, and Kudritzki, 2003), then the final stellar mass M_* is related to the initial protostellar mass M_{pr} by

$$M_*(t) = M_{\text{pr}} + \int_0^t \dot{M}(t) dt. \quad (42)$$

The final mass is therefore determined by the evolution of the mass accretion rate $\dot{M}(t)$ over the lifetime of the star. This in turn is influenced both by the properties of the gas surrounding the star – the amount of gas available, its temperature and angular momentum, etc. – and by the effects of feedback from the star onto the gas, in the form of radiation and outflows.

4.1. ACCRETION IN THE ABSENCE OF FEEDBACK

Protostellar feedback is complicated to model, and so it is easier to begin by considering models of protostellar accretion that do not include its effects. Since feedback will act to reduce the accretion rate, and hence also the final stellar mass, these models allow us to place an upper limit on the ultimate mass scale of the first stars.

One possible approach to determining the accretion rate is to construct a simplified model for the collapsing protostellar core from which an approximation to the true accretion rate can be derived. For instance, if we assume that the protostellar core is isothermal and spherically symmetric, then there exists an entire family of similarity solutions that could potentially be used to describe the collapse (Hunter, 1977; Whitworth and Summers, 1985), of which the most familiar are the Larson-Penston solution (Larson, 1969; Penston, 1969) and the Shu solution (Shu, 1977).

This approach has recently been applied to primordial star formation by Tan and McKee (2004). They model the accretion flow as a spherical, isentropic polytrope, and derive an accretion rate that is a function of three parameters: the entropy parameter $K = p/\rho^\gamma$, the polytropic index γ_p (which, for an isentropic flow, is equal to the adiabatic index γ), and ϕ_* , a numeric parameter of order unity, which is related to the initial conditions of the flow. Tan and McKee normalize these parameters based on the numerical results discussed in the previous sections, and set $\gamma_p = 1.1$, $\phi_* = 1.43$ and $K = 1.88 \times 10^{12} K'$ (in cgs units), where

$$K' = \left(\frac{T_{\text{eff}}}{300 \text{ K}} \right) \left(\frac{n_{\text{H}}}{10^4 \text{ cm}^{-3}} \right)^{-0.1}, \quad (43)$$

and where the effective temperature $T_{\text{eff}} = P_{\text{eff}}/(nk)$ includes the small contribution to the effective pressure made by subsonic turbulence. With these values, the accretion rate becomes⁵

$$\dot{M} = 7.0 \times 10^{-2} K'^{3/2} \left(\frac{t}{1 \text{ yr}} \right)^{-0.30} \text{ M}_{\odot} \text{ yr}^{-1}. \quad (44)$$

This is plotted in figure 3 for the case of $K' = 1$.

Another obvious approach is to simulate the accretion flow numerically, but, as previously discussed, an accurate 3D simulation remains impractical due to the expense of the radiative transfer calculations. We are therefore forced to choose between simulating the radiative transfer and the cooling accurately, at the cost of restricting the hydrodynamics to one dimension, or simulating the hydrodynamics correctly, at the cost of oversimplifying (or simply neglecting) the radiative transfer effects.

Two important examples of the first approach are the simulations of Omukai and Nishi (1998) and Ripamonti *et al.* (2002), discussed at the end of section 3. To recapitulate: Omukai and Nishi use a spherically-symmetric Lagrangian code to simulate protostellar core formation within initially polytropic clouds, and include a thorough treatment of radiative transfer within the H_2 lines and in the continuum, using the tangent ray method (Hummer and Rybicki, 1971). Omukai and Nishi find that prior to core formation the flow is well described by a Larson-Penston type similarity solution; specifically, the solution corresponding to $K = 4.2 \times 10^{11}$ (cgs) and $\gamma = 1.09$. They are unable to continue their simulations after the formation of the protostellar core, as the Courant timestep in the central regions becomes prohibitively small. However, if the same Larson-Penston type solution were to apply after core formation, then the resulting accretion rate would be

$$\dot{M} = 8.3 \times 10^{-2} \left(\frac{t}{1 \text{ yr}} \right)^{-0.27} \text{ M}_{\odot} \text{ yr}^{-1} \quad (45)$$

and the stellar mass would grow as

$$M_* = 0.11 \left(\frac{t}{1 \text{ yr}} \right)^{0.73} \text{ M}_{\odot}. \quad (46)$$

⁵ Strictly speaking, the accretion rate derived by Tan and McKee (2004) is for accretion onto both the protostar and its associated accretion disk. Moreover, they also allow for the possibility that protostellar feedback may reduce the amount of gas reaching the centre of the system. However, for ease of comparison between their results and those of the other authors discussed in this section, I have neglected these complications for the time being.

The simulations of Ripamonti *et al.* (2002) are similar in design to those of Omukai and Nishi (1998), but incorporate several significant improvements. Specifically, Ripamonti *et al.* include:

- (i) A term in the momentum equation corresponding to the radiative force per unit mass

$$f_{\text{rad}} = \frac{1}{c} \int \kappa_{\nu} F_{\nu} d\nu, \quad (47)$$

where κ_{ν} and F_{ν} are the opacity and specific energy flux at frequency ν .

- (ii) An improved treatment of chemistry and thermodynamics at very high densities ($n > 10^{21} \text{ cm}^{-3}$), based on Saumon, Chabrier, and van Horn (1995), that accounts for non-ideal effects such as pressure ionization.
- (iii) A ‘frozen core’ approximation, which keeps the central mass shells fixed in space once their infall velocities fall below a specified value ($v/v_{\text{ff}} < 10^{-3}$) and their temperatures exceed $5 \times 10^4 \text{ K}$. This approximation allows the simulations to avoid the worst of the Courant timestep limitations, and hence enables them to be continued into the period after core formation.

Prior to core formation, there is good agreement between the results of Omukai and Nishi (1998) and Ripamonti *et al.* (2002), confirming that the flow at this initial stage is well described by a Larson-Penston type similarity solution. Differences appear, however, once the protostellar core has formed. For initial conditions comparable to those studied in Omukai and Nishi (1998), Ripamonti *et al.* obtain an accretion rate that is approximately

$$\dot{M} = 6.0 \times 10^{-2} \left(\frac{t}{1 \text{ yr}} \right)^{-0.343} \text{ M}_{\odot} \text{ yr}^{-1}, \quad (48)$$

which is smaller than the Omukai and Nishi rate and falls off more rapidly.

Ripamonti *et al.* also find that the accretion rate is sensitive to the initial conditions of the simulation: clouds with higher initial temperatures produce cores with larger accretion rates, even though the simulations strongly converge at late times. The difference in rates is large enough to produce a difference of a factor of a few in M_* by the end of the simulations, which follow only the first 10 years after core formation. At later times, we would expect the difference to be even more pronounced.

Turning to the ‘hydrodynamical’ approach, the best examples are the simulation by Abel, Bryan, and Norman (2002), discussed in detail in the previous section, and the recent work by Bromm and Loeb (2004). In both cases, the full hydrodynamical problem is solved, using adaptive mesh refinement in the former case, and SPH with particle resampling (Kitsionas and Whitworth, 2002; Bromm and Loeb, 2003) in the latter. Additionally, chemistry and cooling are followed accurately up to the point at which opacity effects begin to dominate. At this point, the two treatments diverge. Abel, Bryan, and Norman halt their simulation once the optical depth at line centre of the main H_2 cooling lines exceeds 10, at which point the maximum gas density is approximately 10^{13} cm^{-3} , and the size of the dense core is a few tens of AU. They estimate the subsequent accretion rate based on a calculation of the accretion timescale, t_{acc} , at the end of their simulation. They take t_{acc} to be

$$t_{\text{acc}} = \frac{M(r)}{\dot{M}(r)} = \frac{M(r)}{4\pi\rho(r)r^2|v_r(r)|}, \quad (49)$$

where v_r is the radial velocity of the gas, and they assume that the stellar mass at time t is simply the mass of gas with $t_{\text{acc}} \leq t$. The resulting inferred accretion rate is plotted in figure 3.

Bromm and Loeb (2004) are also unable to follow the flow to very high densities, since they too neglect opacity effects when calculating their H_2 cooling rate. However, unlike Abel, Bryan, and Norman (2002), they are not forced to halt their simulation once the gas becomes optically thick. Instead, they replace the SPH particles representing the dense, optically thick gas with sink particles of the type described earlier. Sink particle creation is handled much as in Bromm, Coppi, and Larson (2002); the main difference is that the density threshold for sink creation is much higher, being set at $n_{\text{th}} = 10^{12} \text{ cm}^{-3}$. Note that while the code is capable of creating multiple sink particles, in practice only a single sink is required. By using a sink particle, they sacrifice the ability to follow the further evolution of the high density gas, and the ultimate formation of the protostar, but in return can continue to study the gas flow on larger scales for an extended period. On the assumption that all of the gas that is accreted by the sink particle will in reality be accreted by the protostar, they derive a protostellar accretion rate that is approximated by a broken power-law:

$$\dot{M} = \begin{cases} 5.6 \times 10^{-2} \left(\frac{t}{\text{1yr}}\right)^{-0.25} & t \leq 10^3 \text{ yr} \\ 6.3 \times 10^{-1} \left(\frac{t}{\text{1yr}}\right)^{-0.6} & t > 10^3 \text{ yr} \end{cases} \quad (50)$$

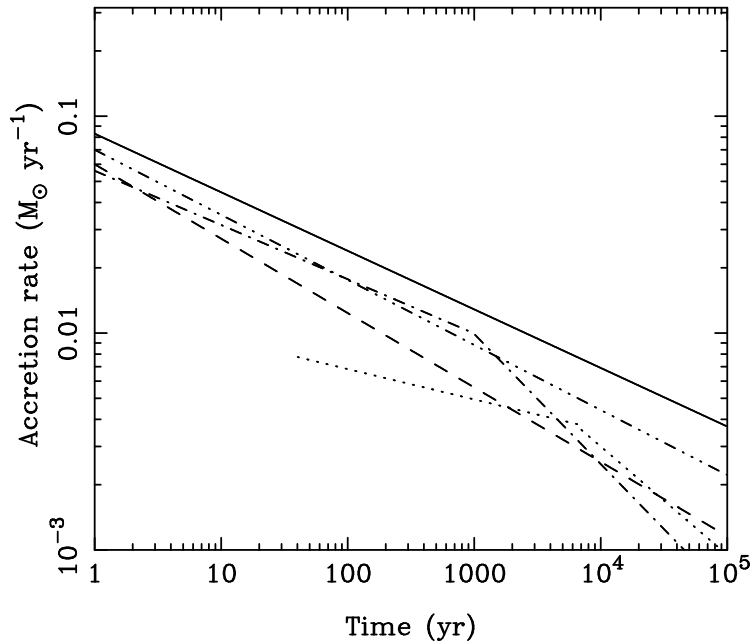


Figure 3. The time-dependent accretion rates predicted by various models of protostellar accretion. Solid line – Omukai and Nishi (1998); dashed line – Ripamonti *et al.* (2002); dotted line – Abel, Bryan, and Norman (2002); dash-dotted line – Bromm and Loeb (2004); dash-dot-dot-dotted line – Tan and McKee (2004). In plotting the Tan and McKee rate, I have assumed $K' = 1$. For $t \lesssim 40$ yr, the predicted accretion rate of Abel, Bryan, and Norman (2002) depends on the behaviour of gas on scales close to or below the resolution limit of their simulation, and is therefore highly uncertain.

Although the two hydrodynamical models agree well at late times (as can be seen by a comparison of their predicted accretion rates, which are plotted in figure 3), at early times there is considerable disagreement, with Bromm and Loeb (2004) predicting a much higher initial accretion rate than Abel, Bryan, and Norman (2002). Unfortunately, with only a single example of each simulation available, it is not possible to say how much of this disagreement can be attributed to the difference in simulation methods, and how much simply reflects natural variation between the accretion rates in different protogalaxies. Further simulations along these lines would clearly be valuable.

An important open question, which has yet to be studied numerically, is what role angular momentum plays in the final stages of accretion onto the protostar. In particular, we would like to know whether angular momentum continues to be transported efficiently outwards, as it is in the simulations of Abel, Bryan, and Norman (2002), or whether it remains approximately constant once the accretion flow

becomes supersonic, as assumed by Tan and McKee (2004). This is important because in the former case the bulk of the accretion will occur directly onto the surface of the protostar, while in the latter case accretion will occur primarily through a circumstellar accretion disk.

By its very nature, this problem is not one that can be tackled using one-dimensional simulations; a full three-dimensional treatment is called for. However, disk formation, if it occurs, will take place after the flow has become optically thick, since the initial disk radius is predicted to be only a few AU (Tan and McKee, 2004). Absent a sudden increase in computing power sufficient to allow us to treat the coupled radiative transfer and hydrodynamics accurately using an algorithm such as that outlined in Hayes and Norman (2003), the best approach is probably to look for some approximate treatment that succeeds in capturing the essential behaviour of the flow, even if this turns out to be somewhat inaccurate. One possible approximation is outlined in Ripamonti and Abel (2004). They derive an H_2 cooling rate for optically thick gas by considering the simplified problem of radiation escaping from a spherically symmetric, collapsing protostellar core. The resulting cooling rate is well fit by

$$L_{\text{H}_2,\text{thick}}(T) = L_{\text{H}_2,\text{thin}}(T) \min\left(1, (n/n_0)^{-\beta}\right), \quad (51)$$

where $n_0 = 8 \times 10^9 \text{ cm}^{-3}$, $\beta = 0.45$, and where $L_{\text{H}_2,\text{thin}}(T)$ is the H_2 cooling rate in optically thin gas. Ripamonti and Abel demonstrate that this simple approximation performs well in comparison to the full radiative transfer solution used in Ripamonti *et al.* (2002); however, its accuracy in the three dimensional case is currently unknown. More work along these lines is clearly called for if we are to make progress on solving this challenging problem.

Nevertheless, despite the gaps that remain in our understanding of primordial accretion flows, one point stands out clearly: the predicted accretion rates are very much larger than those inferred for local protostars, which are typically of the order of 10^{-4} – $10^{-5} M_{\odot} \text{ yr}^{-1}$ for class 0 objects (see, e.g. Maret *et al.*, 2002; Beuther *et al.*, 2002), and which decrease significantly as the protostar evolves (André, Ward-Thompson, and Barsony, 2000).

The reason for this difference is straightforward. On purely dimensional grounds, we would expect the time taken to accrete a mass M of gas to be of the order of the free-fall timescale for the gas, unless some other effect, such as magnetic support or protostellar feedback, were to retard the collapse. Therefore, we can write the *mean* accretion rate for the gas as

$$\dot{M} \propto \frac{M}{t_{\text{ff}}}, \quad (52)$$

where we expect the constant of proportionality to be of order unity. For gas with a mean density $\bar{\rho}$, we have $t_{\text{ff}} \propto \bar{\rho}^{-1/2}$, and hence

$$\dot{M} \propto M \bar{\rho}^{1/2}. \quad (53)$$

Now, if this mass of gas is close to being in hydrostatic equilibrium, which the results of Abel, Bryan, and Norman (2002) show is a reasonable approximation for the gas surrounding the protostellar core, then M must be of the order of the Jeans mass; if $M \ll M_{\text{J}}$, the gas would not be collapsing, while if $M \gg M_{\text{J}}$, it would almost certainly have fragmented. Therefore, the accretion rate scales as

$$\dot{M} \propto M_{\text{J}} \bar{\rho}^{1/2}, \quad (54)$$

or, since $M_{\text{J}} \propto (T^3/\bar{\rho})^{1/2}$,

$$\dot{M} \propto T^{3/2}. \quad (55)$$

Since the minimum temperature reached by the primordial gas is more than an order of magnitude larger than the temperature characteristic of local prestellar cores (which is typically of order 10 K; see Ward-Thompson, André, and Kirk, 2002), we would expect the accretion rate to be correspondingly greater, which is precisely what we find in the detailed models discussed above.

In the absence of significant protostellar feedback, these large predicted accretion rates will lead to large final stellar masses. This is clearly demonstrated in figure 4, where I plot the final stellar mass as a function of time for all of the models discussed above. In every case, the final stellar mass grows to more than $100M_{\odot}$ in less than 10^5 yr. Therefore, unless feedback from the protostar can significantly reduce the amount of material that the star accretes over its lifetime, it will inevitably become very massive, and will either end its life as a pair-instability supernova (if its final mass lies in the range $140 < M < 260 M_{\odot}$), or by collapsing directly to form a black-hole (Fryer, Woosley, and Heger, 2001; Heger *et al.*, 2003). The possible consequences of this are discussed in some detail by Yoshida, Bromm, and Hernquist (2004) and I will not discuss them here.

4.2. MODELING PROTOSTELLAR FEEDBACK

Any potential form of feedback will be powered, directly or indirectly, from one of two sources: the energy released by the infalling matter, or the energy produced by nuclear burning within the protostar. To model the former, we must model gas flow near the surface of the protostar, paying particular attention to the properties of the accretion shock and

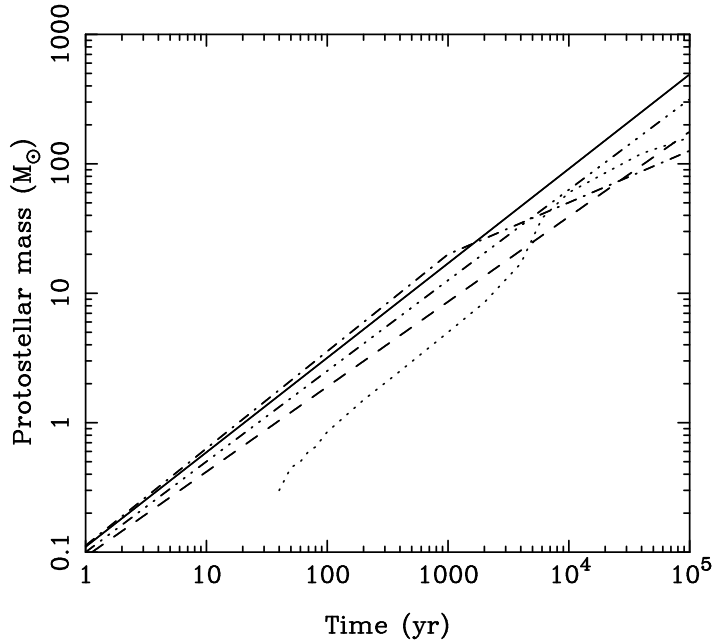


Figure 4. The time-dependent protostellar masses produced by the accretion rates shown in figure 3.

the circumstellar accretion disk. To model the latter, we must model the internal structure of the protostar. In practice, since the dominant energy source will change over time, from accretion at early times to nuclear burning at late times, an ideal model should treat both regions, together with as much of the surrounding gas as possible.

Unfortunately, computational limitations again restrict us to more limited models, and we are forced to approximate. The most significant approximation that is commonly made is the assumption of spherical symmetry. This is a reasonable approximation for the protostar itself, provided rotational effects are not significant, but it does not allow us to treat any processes involving the accretion disk, and is therefore rather limiting. On the other hand, it dramatically reduces the computational requirements of the problem, and consequently continues to be a widely used approximation. Indeed, the only treatment of primordial protostellar structure and feedback of which I am aware that does not assume spherical symmetry is the recent work of Tan and McKee (2004) and Tan and Blackman (2004), which is discussed in some detail later in this section.

It is also common to further simplify the problem by splitting it into two pieces, and considering the evolution of the structure of the protostar (which will strongly influence the strength of any feedback)

separately from the effect of feedback on the flow. In other words, studies of protostellar structure generally assume a constant accretion rate, while calculations focused on the effects of feedback on the accretion flow frequently assume a constant energy source. This separation is purely pragmatic; it is easier to study the different processes separately before combining them in more realistic coupled models.

4.2.1. *The evolution of protostellar structure*

The evolution in the structure of a primordial protostar as it accretes matter from its surroundings was first studied in detail by Stahler, Palla, and Salpeter (1986a). Their strategy followed that of Stahler, Shu, and Taam (1980ab, 1981), who had previously studied a similar problem for the case of a low-mass, population I star.

They assume that the accretion process can be treated as a series of quasi-steady-state accretion flows onto a hydrostatic core, which is bounded by a strongly radiating accretion shock. Within the core, the standard stellar structure equations are solved, with the assumption that deuterium burning is the only source of nuclear energy. Outside the core, the treatment depends on the optical depth of the gas. If the gas is optically thin to the radiation from the accretion shock, then the accretion flow is assumed to be in free-fall. Otherwise, a more detailed calculation is made that incorporates the effects of the radiation force on the infalling gas. The accretion shock itself is treated as a simple discontinuity; no attempt is made to model its structure in any detail. Since the thickness of the shock is small compared to the size of the core, this should be a good approximation.

Stahler, Palla, and Salpeter (1986a) begin with an initial core mass of $0.01 M_{\odot}$, and give the core an arbitrary initial distribution of specific entropy:

$$s(M) = s_0 + \beta \frac{k}{m_{\text{H}}} \left(\frac{M}{M_{\odot}} \right)^2, \quad (56)$$

where $\beta = 7.39$ and s_0 is calculated from the adopted central temperature ($T_{\text{c}} = 10^5$ K) and density ($\rho_{\text{c}} = 0.28$ g cm $^{-3}$) using an equation of state taken from Eggleton, Faulkner, and Flannery (1973). The outer boundary condition is fixed by the accretion rate, which Stahler, Palla, and Salpeter take to be constant, with a value $4.41 \times 10^{-3} M_{\odot} \text{ yr}^{-1}$.

Starting from these initial conditions, Stahler, Palla, and Salpeter calculated the subsequent evolution of the protostar until the core mass reached a value of $10.5 M_{\odot}$. They found that the evolution could be divided into three qualitatively distinct phases.

In the first phase, which lasts until the core mass reaches $0.1 M_{\odot}$, the protostar relaxes from its initial entropy profile into one appropriate for the particular choice of accretion rate. This ‘decay of transients’ phase

indicates that although the initial conditions are probably incorrect in detail, the flow soon loses all memory of them, and therefore any inaccuracy at this stage is unlikely to affect the later results.

Once the initial transients have died away, the protostar enters the second phase of its evolution. During this phase, its central temperature remains low ($T_c \sim 10^5$ K), resulting in a high interior opacity and hence a low interior luminosity. Consequently, the evolution of the core during this phase is almost adiabatic; although the core continues to gradually contract, this contraction does not lead to any increase in the central entropy. Since the postshock entropy increases over time due to the increasing strength of the accretion shock (which is itself a natural result of the increasing protostellar mass), the core develops an off-centre distribution of entropy and temperature.

The gas surrounding the accretion shock remains optically thick throughout this period. This is a direct result of the high accretion rate, which produces a highly luminous accretion shock. This produces sufficient radiation to partially ionize the preshock gas in the vicinity of the shock, creating a structure known as a radiative precursor. The H^- opacity of the dense, partially ionized gas in this radiative precursor is more than sufficient to make it optically thick. Stahler, Palla, and Salpeter show that the core radius during this period evolves as

$$R_* = 48.1 \left(\frac{M_*}{M_\odot} \right)^{0.27} \left(\frac{\dot{M}}{\dot{M}_0} \right)^{0.41} R_\odot, \quad (57)$$

where $\dot{M}_0 = 4.41 \times 10^{-3} M_\odot \text{yr}^{-1}$, while the photospheric radius evolves as

$$R_p = 66.8 \left(\frac{M_*}{M_\odot} \right)^{0.27} \left(\frac{\dot{M}}{\dot{M}_0} \right)^{0.41} R_\odot, \quad (58)$$

so $R_p > R_*$ throughout. The strong H^- opacity also keeps the photospheric temperature low ($T_p \sim 5000$ K), which prevents the protostar from being able to ionize material outside of its photosphere.

This near-adiabatic accretion phase comes to an end once the cooling time of the core, given approximately by the Kelvin-Helmholtz timescale

$$t_{\text{KH}} = \frac{GM_*^2}{R_*L_*}, \quad (59)$$

becomes comparable to the accretion timescale $t_{\text{acc}} = M_*/\dot{M}$. This occurs for a core mass $M \sim 1M_\odot$, and results in the core entering a phase of homologous collapse, while energy and entropy are transferred outwards in the form of a ‘luminosity wave’. The radial position of the luminosity peak moves outwards towards the accretion shock, reaching

it at about the time that the core mass has reached $8 M_{\odot}$. This results in a rapid swelling of the outermost layers, which weakens the accretion shock and leads to it becoming optically thin. Stahler, Palla, and Salpeter terminate their simulation shortly afterwards, once the core mass has reached $10.5 M_{\odot}$.

Although Stahler, Palla, and Salpeter include deuterium burning as a possible energy source, in practice they find that it plays no role at this stage of the protostar's evolution, as its central temperature remains too low to ignite deuterium. However, since the central temperature and density are both rising sharply at the end of the simulation as the central regions of the core collapse homologously, it is reasonable to assume that deuterium ignition will soon take place. Stahler, Palla, and Salpeter (1986b) study the onset of deuterium burning and the later onset of hydrogen burning in a subsequent simulation of the pre-main sequence evolution of a $5 M_{\odot}$ primordial protostar. Their initial conditions are taken from Stahler, Palla, and Salpeter (1986a), but the accretion rate is now set to zero. Stahler, Palla, and Salpeter (1986b) find that deuterium ignites approximately 6000yr after the beginning of their simulation, with hydrogen ignition following after 2×10^5 yr. The protostar eventually reaches the zero-age main sequence approximately 10^6 yr into the simulation.

An alternative treatment of these later stages of evolution that does not assume a negligible accretion rate is that of Omukai and Palla (2001). They construct their simulation in the same way as Stahler, Palla, and Salpeter (1986a) and assume the same constant rate. The only significant technical differences between the two simulations are that Omukai and Palla use zero metallicity opacities from Lenzuni, Chernoff, and Salpeter (1991) and Iglesias and Rogers (1996) in place of the older values used by Stahler, Palla, and Salpeter, and that they begin their simulation at the start of the optically thin phase, when the core mass has already reached $M = 8 M_{\odot}$. However, unlike Stahler, Palla, and Salpeter, they do not halt their simulation once the core mass reaches $10.5 M_{\odot}$; instead, they continue until well after hydrogen ignition.

They find that the period of optically thin evolution identified by Stahler, Palla, and Salpeter (1986a) lasts for only a short time; the core reaches a maximum radius of $220 R_{\odot}$ for a core mass of $11.5 M_{\odot}$, but shortly afterwards begins a sustained process of contraction. The radiative precursor reappears once the core mass reaches $12.4 M_{\odot}$ and persists for the remainder of the simulation. As in the previous optically thick phase, H^{-} opacity keeps the photospheric temperature low.

Within the core, deuterium burning begins once the mass of the core reaches $12 M_{\odot}$ (corresponding to a time $t = 1000$ yr after the beginning

of the simulation, given the assumed accretion rate), and is complete by the time the mass has reached $30M_{\odot}$ (corresponding to $t = 5000\text{yr}$). It does not contribute significantly to the protostellar luminosity, and has little effect on the structure of the protostar.

Hydrogen ignition follows once the core mass reaches $80 M_{\odot}$ (corresponding to $t = 1.6 \times 10^4 \text{yr}$). At the same time, the internal luminosity nears the Eddington value

$$L_{\text{Edd}} = \frac{4\pi cGMm_{\text{p}}}{\sigma_{\text{T}}} \quad (60)$$

$$= 1.26 \times 10^{38} \left(\frac{M}{M_{\odot}} \right) L_{\odot}, \quad (61)$$

triggering a second phase of expansion. The outer layer of the core moves out from $10 R_{\odot}$ to $100 R_{\odot}$, although it remains well within the photosphere, which has a radius of approximately $1000 R_{\odot}$ at this time. As the core expands, the accretion luminosity falls and the radiation force on the outer layers of the core declines. It soon becomes too small to maintain the expansion, and so the core begins to contract rapidly for a second time. From this point on, however, nuclear burning makes a substantial and increasing contribution to the total protostellar luminosity, which soon reaches L_{Edd} for a second time. This triggers another phase of radiation-driven expansion, which this time is strong enough to halt the accretion. This occurs once the core mass has reached $M \sim 300 M_{\odot}$, and Omukai and Palla terminate their simulation at this point.

In order to assess the dependence of this result on the adopted accretion rate, Omukai and Palla (2003) performed a similar analysis for a range of different values of \dot{M} . They defined a fiducial accretion rate $\dot{M}_{\text{fid}} = 4.41 \times 10^{-3} M_{\odot} \text{yr}^{-1}$ corresponding to the value adopted by Stahler, Palla, and Salpeter (1986a) and Omukai and Palla (2001), and studied models with rates $\dot{M} = (0.25, 0.5, 1.0, 2.0) \times \dot{M}_{\text{fid}}$, as well as a model using the time-dependent accretion rate predicted by Abel, Bryan, and Norman (2002).

The earliest stages of protostellar evolution are qualitatively the same in all of these models: we see the same sequence of adiabatic growth, propagation of a luminosity wave that triggers expansion of the outer layers, followed by rapid contraction. There *are* quantitative differences; for instance, protostars with a larger \dot{M} have a larger radius at a given mass. However, significant differences in behaviour do not become apparent until the end of the rapid contraction phase. In the fiducial case, Omukai and Palla (2003) confirm their previous result: they find two episodes of radiation-driven expansion, the second of which is strong enough to terminate accretion onto the protostar. In the

$\dot{M} = 2\dot{M}_{\text{fid}}$ case, however, they find that the initial phase of expansion is strong enough to halt the accretion, thanks to the larger accretion luminosity associated with the larger accretion rate. Consequently, the final protostellar mass is smaller, being approximately $90 M_{\odot}$.

In the two models with $\dot{M} < \dot{M}_{\text{fid}}$, however, the outcome is rather different. Core contraction comes to an end shortly after the onset of hydrogen burning, but there is no subsequent phase of radiation-driven expansion, as the protostellar luminosity is never more than 70% of L_{Edd} . Instead, the core relaxes quickly onto the zero-age main sequence (ZAMS), continuing to accrete all the while.

Omukai and Palla (2003) show that there is a critical accretion rate \dot{M}_{crit} that separates these two outcomes. Protostars with $\dot{M} < \dot{M}_{\text{crit}}$ can reach the zero-age main sequence while still accreting, and can therefore grow to extremely large masses, while protostars with $\dot{M} > \dot{M}_{\text{crit}}$ will undergo radiation-driven expansion before reaching the ZAMS, and will therefore have smaller masses. To evaluate \dot{M}_{crit} , Omukai and Palla equate the total luminosity of a protostar that has just reached the ZAMS with the Eddington luminosity:

$$L_{\text{Edd}} = L_{\text{ZAMS}} + \frac{GM_*\dot{M}_{\text{crit}}}{R_{\text{ZAMS}}}, \quad (62)$$

where the second term on the right-hand side represents the accretion luminosity. This equation can be rewritten as

$$\dot{M}_{\text{crit}} = \frac{4\pi c R_{\text{ZAMS}}}{\kappa_{\text{es}}} \left(1 - \frac{L_{\text{ZAMS}}}{L_{\text{Edd}}} \right), \quad (63)$$

where κ_{es} is the electron scattering opacity. Evaluating this, we find that $\dot{M}_{\text{crit}} \simeq 4 \times 10^{-3} M_{\odot} \text{yr}^{-1}$, coincidentally close to \dot{M}_{fid} . In principle, \dot{M}_{crit} has a dependence on the mass of the protostar, but in practice this dependence is weak and may be neglected.

The final model that Omukai and Palla (2003) consider is one with a time-dependent accretion rate taken from Abel, Bryan, and Norman (2002). In this model, the accretion rate is initially much larger than \dot{M}_{crit} , but decreases with time, and falls below \dot{M}_{crit} when the core mass reaches $95 M_{\odot}$. This initial behaviour of this model is very similar to that of the model with $\dot{M} = \dot{M}_{\text{fid}}$, but the two diverge during the rapid contraction phase; the time dependent model undergoes a very brief period of radiation-driven expansion, but thereafter re-contracts, and relaxes onto the zero-age main sequence, following which its evolution is indistinguishable from that of the other models with $\dot{M} < \dot{M}_{\text{crit}}$.

An alternative view of the evolution of protostellar structure is presented by Tan and McKee (2004). In contrast to previous authors, they do not assume spherical symmetry, allowing them to treat the case of

accretion via a circumstellar disk. Tan and McKee fix the size of the disk by assuming that angular momentum is conserved by gas within the sonic point of the accretion flow. This allows them to write the disk radius as

$$r_d = f_{\text{Kep}}^2 \left(\frac{M_{\text{sp}}}{m_{*d}} \right) r_{\text{sp}}, \quad (64)$$

where r_{sp} is the radius of the sonic point, M_{sp} is the mass interior to the sonic point, m_{*d} is the mass interior to r_d (i.e. the mass of the protostar plus the disk) and f_{Kep} is the ratio of the rotational velocity of the gas to the Keplerian orbital velocity $v_{\text{Kep}} = (GM/r)^{1/2}$, evaluated at the sonic point. Tan and McKee fix r_{sp} using their analytic accretion flow solution, discussed in the previous section, and adopt $f_{\text{Kep}} = 0.5$, based on the results of Abel, Bryan, and Norman (2002). They show that in this case, the accretion disk radius becomes

$$r_d = 3.44 \left(\frac{f_{\text{Kep}}}{0.5} \right)^2 \epsilon_{*d}^{-9/7} \left(\frac{m_{*d}}{M_\odot} \right)^{9/7} K'^{-10/7} \text{ AU}, \quad (65)$$

where K' is given by Equation (43), and where ϵ_{*d} is the fraction of the infalling gas that reaches the disk or the star. In the absence of protostellar feedback, $\epsilon_{*d} = 1$.

Provided that $r_d \gg r_*$, which will generally be the case, the bulk of the gas will accrete first onto the disk and only later onto the protostar. Therefore, the accretion rate onto the protostar, and hence its structure, will be determined in large part by the behaviour of the disk. To determine the disk structure, Tan and McKee (2004) use the standard theory of steady, thin viscous accretion disks (as outlined in Shakura and Sunyaev, 1973 or Frank, King, and Raine, 1995), with a spatially constant viscosity parameter α . The dominant source of this viscosity and the appropriate value for α remain uncertain, much as they do in the analogous situation in present-day star formation. Possible sources of viscosity include gravitational instabilities within the disk (Larson, 1984; Lin and Pringle, 1987; Bodenheimer, 1995; Nomura and Mineshige, 2000; Gammie, 2001; Johnson and Gammie, 2003), tidal interactions with external mass concentrations (Spruit, 1987; Larson, 1990; Lin and Papaloizou, 1993; Blondin, 2000; Larson, 2002), and turbulence generated by the magnetorotational instability (MRI; see Balbus and Hawley, 1991, 1998)

The last of these will only operate if a sufficiently strong magnetic field is present in the disk. Kulsrud *et al.* (1997) showed that a very small seed field could be produced via the Biermann battery mechanism (Biermann, 1950) during the collapse of the protogalactic gas, and Tan and Blackman (2004) show that although this field is initially too small to drive the MRI, a dynamo process acting in the disk will

rapidly amplify the field, which soon becomes strong enough to drive the instability. In view of this, Tan and McKee (2004) examine the behaviour of a disk with $\alpha = 0.01$, the appropriate value for a disk susceptible to MRI (Balbus and Hawley, 1998).

Having determined the disk structure and the rate at which gas accretes from the disk onto the protostar, Tan and McKee (2004) then solve for the evolution of the protostellar structure using a modified version of the analytic approach developed by Nakano, Hasegawa, and Norman (1995) and Nakano *et al.* (2000). In this approach, the protostellar radius is found balancing the rate of accretion of energy with the rate of change of the total protostellar energy. The internal structure of the protostar is not solved for explicitly; instead, it is approximated as a polytrope, with the polytropic index fixed by comparison with the results of Stahler, Palla, and Salpeter (1986a) and Omukai and Palla (2001).

Tan and McKee (2004) show that if an accretion disk is not present (i.e. if $f_{\text{Kep}} = 0$), and if $\dot{M} = \dot{M}_{\text{fid}}$, then this model successfully reproduces the results of Stahler, Palla, and Salpeter (1986a) and Omukai and Palla (2001). They also demonstrate that the presence of a disk has a relatively small effect on the evolution of the protostar. The protostellar radius tends to be somewhat larger than in the spherical accretion case, but the protostar still evolves through the same progression of adiabatic growth, terminated by the emergence of a luminosity wave, followed by rapid contraction that ends once the protostar reaches the zero-age main sequence. The major difference from the spherical case is in the behaviour of the photosphere. Because most of the gas accretes onto the protostar via the disk, the gas density is significantly reduced in regions near the protostar but out of the plane of the disk. Consequently, the optical depth of these regions is also significantly reduced, with the result that the flow becomes optically thin early in its evolution. For example, in the model with $f_{\text{Kep}} = 0.5$, the photosphere vanishes once the protostellar mass reaches $1 M_{\odot}$ and does not subsequently reappear. As we will see below, this may have a major influence on the effectiveness of radiative feedback from the protostar.

4.2.2. *The effects of feedback*

In order for the protostar to substantially reduce the rate at which it accretes, it must be able to transfer a significant amount of energy and/or momentum to the infalling gas. A number of possible mechanisms that accomplish this have been suggested, which fall under two broad headings: *radiative feedback*, where radiation from the protostar (or the accretion disk) is responsible for transferring energy and momentum directly to the infalling gas, and *mechanical feedback*, where

the protostar transfers energy and momentum to some form of outflow, which subsequently transfers it to the infalling material.

In local star-forming regions, the dominant mechanism is a form of radiative feedback: radiation pressure exerted on the infalling dust grains by the protostar results in a substantial momentum transfer to the gas and prevents massive stars from forming, unless the accretion rate is very large (Wolfire and Cassinelli, 1987). In dust-free primordial gas, however, this process is clearly inoperative, and we must examine other possibilities.

One obvious possibility is that radiation within the optically thick rotational and vibrational lines of H_2 may exert sufficient pressure to slow or stop the infall. However, this seems unlikely to be the case: in their simulation of protostellar formation, Ripamonti *et al.* (2002) compute the total opacity of the H_2 lines and show that it is never more than 5% of the electron scattering opacity, implying that the protostar would have to radiate a total luminosity in the H_2 lines that was many times larger than the Eddington luminosity for this effect to be dynamically significant.

A more interesting possibility is that the buildup of an H II region around the protostar may terminate the accretion. This idea was first discussed in the context of present day star formation by Larson and Starrfield (1971), and was re-examined in the context of primordial star formation by Omukai and Inutsuka (2002). The basic mechanism is straightforward: as the protostar ionizes the gas, it transfers to it a considerable amount of thermal energy. If the H II region can expand to a radius at which this thermal energy exceeds the gravitational binding energy of the gas, then the ionized gas outside this radius will become unbound from the central protostar, and little if any of it will ultimately be accreted. To assess the effectiveness of this mechanism, we need to answer two basic questions: one, does an H II region actually form? And two, if an H II region does form, can it expand sufficiently to unbind the gas, or will it instead be confined to a small radius by the inflow?

The answer to the first of these questions will depend on the effective temperature of the protostar. An isolated, massive metal-free star on the main sequence will have an effective temperature of approximately 10^5 K (Cojazzi *et al.*, 2000), and will emit a substantial number of ionizing photons, so in this case it is clear that an H II region will form. On the other hand, in the accretion models of Stahler, Palla, and Salpeter (1986a) and Omukai and Palla (2001, 2003) discussed in the previous section, the protostar is hidden within a much larger photosphere, with an effective temperature of only 6000 K, and so no H II region will form until the photosphere vanishes at late times.

Regarding the second question, Omukai and Inutsuka (2002) show that if the accretion flow onto the protostar is steady and spherically symmetric, then an H II region can expand sufficiently to unbind the surrounding gas only if it is powered by a flux of ionizing photons that exceeds a critical value, Q_{crit} . They demonstrate that in order to calculate Q_{crit} correctly, it is necessary to take into account an additional type of radiative feedback – the force arising due to radiation scattering within the H II region. There are two main components to this force. One is due to Thomson scattering, and will be negligible until the protostellar luminosity approaches L_{Edd} . The other comes from the momentum transfer that occurs during photoionization, and for a gas in photoionization equilibrium the force per unit mass is given by (Haehnelt, 1995)

$$F_{\text{rad}} = \frac{h\nu_{\text{ion}}}{c} \alpha_{\text{B}} \frac{n_{\text{e}} n_{\text{H}^+}}{\rho}, \quad (66)$$

where α_{B} is the case B recombination coefficient and $h\nu_{\text{ion}} \simeq 13.6$ eV is the mean energy of an ionizing photon. This radiative force acts to reduce the infall velocity within the H II region, which leads to an increase in the density of the ionized gas, since the assumption of steady flow implies that $\rho \propto v^{-1}$, where v is the infall velocity. This increased density leads in turn to a higher recombination rate, which limits the expansion of the H II region. Omukai and Inutsuka show that the net effect is to make Q_{crit} very large; they find a value

$$Q_{\text{crit}} = 6.4 \times 10^{52} \left(\frac{R_{\text{in}}}{10 R_{\odot}} \right)^{-1} \left(\frac{M}{100 M_{\odot}} \right)^2, \quad (67)$$

where R_{in} is the inner radius of the H II region. For reasonable values for the stellar parameters, this gives a value of Q_{crit} that is about a hundred times larger than the actual ionizing flux, suggesting that even if an H II region forms, it will be unable to halt accretion onto the protostar. It is worth noting, however, that the evolution of the H II region is likely to be very sensitive to the density distribution near the protostar and it is not clear that this conclusion will still hold if we relax some of the simplifying assumptions made above. It would be instructive to redo this calculation using a more realistic dynamical model.

A final form of radiative feedback that has attracted serious consideration is the scattering of Lyman- α photons by the infalling gas. Within the H II region, this is of only minor importance, but in the surrounding H I gas, where the optical depth to Lyman- α scattering is much higher, it may be far more significant (Braun and Dekel, 1989; Bithell, 1990; Haehnelt, 1995). Doroshkevich and Kolesnik (1976) argue that the radiation pressure exerted by the Lyman- α photons

will rapidly expel all of the H I gas near the protostar, thereby limiting the final stellar mass to $10 M_{\odot}$ or less. On the other hand, Omukai and Inutsuka (2002) contend that their treatment overestimates the density of Lyman- α photons and so overestimates the effectiveness of this mechanism. More recently, Tan and McKee (2003) have presented preliminary results from a calculation of the effects of Lyman- α scattering that assumes a rotating, axisymmetric inflow. Their results appear to support the Doroshkevich and Kolesnik (1976) picture, although they quote a larger mass limit of order $20 M_{\odot}$. However, full details of their calculations have not yet been published, so it is not possible to assess the strength of their argument.

The effects of feedback in the form of protostellar outflows have been less well studied than the various radiative effects discussed above. In the case of radiatively driven outflows, such as stellar winds from O type stars, this neglect is easy to understand – these outflows are driven primarily by the scattering of photons in the resonance lines of metal ions, and thus grow substantially weaker as the metallicity declines (Kudritzki, 2002). In primordial gas, outflows of this type must rely on Thomson scattering and thus will only become significant if the protostellar luminosity reaches L_{Edd} , which, as we have seen, will only occur if the accretion rate exceeds \dot{M}_{crit} .

Meanwhile, bipolar outflows of the kind that are ubiquitous in local star-forming regions have attracted little study because they are widely believed to be hydromagnetic in nature (see, e.g. Matzner and McKee, 1999) and protogalactic magnetic fields were thought to be too weak to power them. However, in a recent paper, Tan and Blackman (2004) have argued that the initial protogalactic magnetic field will undergo substantial amplification by a helical dynamo operating in the turbulent accretion disk surrounding the protostar, and may therefore become strong enough to drive an outflow. For a reasonable choice of parameters, they find that an outflow with mechanical luminosity

$$L_{\text{mech}} \simeq 100 \left(\frac{M}{M_{\odot}} \right) \left(\frac{\dot{M}}{10^{-2} M_{\odot} \text{ yr}^{-1}} \right) L_{\odot} \quad (68)$$

can be produced. Although this value is substantially less than the radiative luminosity of the protostar, the outflow is far more effective than the radiation at transferring momentum to the surrounding gas. Tan and Blackman estimate that it will begin to remove a significant quantity of gas from the core once the protostellar mass exceeds $20 M_{\odot}$, and that as much as 50% of the core mass may have been removed by the time that the protostellar mass reaches $100 M_{\odot}$. The outflow will also alter the density structure of the core and should therefore be taken into account when assessing the effectiveness of radiative feedback.

4.3. SUMMARY

Although much work remains to be done on developing a detailed understanding of primordial protostellar accretion, several key points are already clear. First, the mean accretion rate of a primordial protostar is much larger than that of its present-day counterparts, simply as a result of the higher gas temperature of the protostellar core. Second, a large quantity of gas is available to be accreted by the protostar, since the very low efficiency of fragmentation means that it does not have to compete with a large number of other protostars for the available gas. Third, many of the forms of protostellar feedback that serve to limit the masses of protostars forming at the present day either do not operate in the primordial case, or operate with a reduced effectiveness. At the same time, the higher accretion rate implies a larger ram pressure of the infalling gas, making the job of halting the accretion harder than at the present day. Fourth, those forms of feedback that do seem to be effective (Lyman- α scattering, hydromagnetic outflows) do not become so until late times, after the protostar has already accreted a substantial quantity of gas.

Taken together, these points strongly suggest that the first stars will be very massive. Indeed, if this basic picture is correct, it is difficult to see how accretion could be terminated early enough to produce a solar mass star, since the predicted accretion rates discussed earlier suggest that this mass of gas will build up in only 10–20 yr.

The major uncertainties that remain are easily summarized:

- (i) Is our basic picture of a single protostar per core correct, or does a second stage of fragmentation occur at late times, after the gas has become optically thick?
- (ii) Does a dynamically significant disk form? If so, how does it evolve, and how does it affect accretion onto the protostar?
- (iii) Is the effective temperature of the protostar 6000 K (as suggested by the models of Stahler, Palla, and Salpeter, or Omukai and Palla) or 10^5 K (as suggested by the models of Tan and McKee)?
- (iv) Are there other possible forms of feedback that we haven't yet considered?

As with many of the open questions concerning primordial star formation, resolution of these issues is likely to require detailed numerical simulations with an adequate treatment of the effects of radiative transfer.

5. Conclusion

The past ten years have seen significant advances in our knowledge of many aspects of primordial star formation, from the large scale environment in which it occurs to the very small scale structure of the first protostellar core. Although a number of issues remain unresolved, a consensus now exists on the broad outlines of the process.

We expect the first stars to form in small, H_2 -cooled protogalaxies, with masses of 10^5 – $10^6 M_\odot$, at redshifts $z = 30$ – 40 . Fragmentation of the gas within these protogalaxies will be inefficient, contrary to previous expectations, and in the smallest protogalaxies only a single dense core will form, with a mass of a few hundred solar masses.

This core will collapse without fragmenting further until it becomes optically thick. Its subsequent evolution is not entirely certain, but the most probable outcome is the formation of a single low-mass protostar near its centre. This protostar will accrete gas rapidly from its surroundings, and will soon become very large. Protostellar feedback may act to limit the accretion rate at late times, in which case the final mass of the star will be similar to that of a Galactic O type star; otherwise, the final stellar mass will be limited only by the amount of gas available, and will be of the order of a few hundred solar masses. The first stars will therefore end their lives either exploding as supernovae, or collapsing directly to form black holes. Either way, there should be none left alive at the present day.

The future also holds great promise for the study of primordial star formation. New facilities such as ALMA and JWST will for the first time allow us to probe the earliest epochs of star formation, and may allow us to test observationally the picture that I have outlined above (although the practical difficulties will remain formidable). Meanwhile, further increases in computing power will allow us to perform increasingly detailed simulations and should soon allow us to fill in many of the gaps in our current understanding of the formation of the first stars.

Acknowledgements

The author acknowledges useful discussions on various aspects of primordial star formation with T. Abel, P. Brand, V. Bromm, G. Bryan, M.-M. Mac Low, M. Norman, and R. Larson. He would also like to thank the referee, V. Bromm, for a careful reading of the manuscript and a number of suggestions which have helped to improve its clarity. Financial support for this work was provided by NSF grants AST99-85392 and AST-0307793, and by NASA Education grant NAG5-13028.

This research has made substantial use of NASA's Astrophysics Data System.

References

- Abel, T., Bryan, G. L., and Norman, M. L.:2000, *Astrophys. J.*, **540**, 39.
- Abel, T., Bryan, G. L., and Norman, M. L.:2002, *Science*, **295**, 93.
- Abel, T., Anninos, P., Zhang, Y., and Norman, M. L.:1997, *New Astron.*, **2**, 181.
- Abel, T., Anninos, P., Norman, M. L., and Zhang, Y.:1998, *Astrophys. J.*, **508**, 518.
- André, P., Ward-Thompson, D., and Barsony, M.:2000, in V. Mannings, A. P. Boss, and S. S. Russell (eds.), *Protostars and Planets IV*, University of Arizona Press, Tucson, U.S.A., p. 59.
- Anninos, P., Norman, M. L., and Clarke, D. A.:1994, *Astrophys. J.*, **436**, 11.
- Anninos, P., Zhang, Y., Abel, T., and Norman, M. L.:1997, *New Astron.*, **2**, 209.
- Arny, T. T.:1966, *Astrophys. J.*, **145**, 572.
- Bahcall, N. A., Ostriker, J. P., Perlmutter, S., and Steinhardt, P. J.:1999, *Science*, **284**, 1481.
- Balbus, S. A. and Hawley, J. F.:1991, *Astrophys. J.*, **376**, 214.
- Balbus, S. A. and Hawley, J. F.:1998, *Rev. Mod. Phys.*, **70**, 1.
- Barkana, R. and Loeb, A., 2001, *Phys. Rep.*, **349**, 125.
- Bate, M. R. and Burkert, A.:1997, *Monthly Not. Roy. Astron. Soc.*, **288**, 1060.
- Bate, M. R., Bonnell, I. A., and Bromm, V.:2003, *Monthly Not. Roy. Astron. Soc.*, **339**, 577.
- Bate, M. R., Bonnell, I. A., and Price, N. M.:1995, *Monthly Not. Roy. Astron. Soc.*, **277**, 362.
- Bennett, C. L., Halpern, M., Hinshaw, G., Jarosik, N., Kogut, A., Limon, M., Meyer, S. S., Page, L., Spergel, D. N., Tucker, G. S., *et al.*:2003, *Astrophys. J. Suppl.*, **148**, 1.
- Benson, A. J., Frenk, C. S., Baugh, C. M., Cole, S., and Lacey, C.:2001, *Monthly Not. Roy. Astron. Soc.*, **327**, 1041.
- Beuther, H., Schilke, P., Sridharan, T. K., Menten, K. M., Walmsley, C. M., and Wyrowski, F.:2002, *Astron. Astrophys.*, **383**, 892.
- Biermann, L.:1950, *Z. Naturforsch*, **5a**, 65.
- Bithell, M.:1990, *Monthly Not. Roy. Astron. Soc.*, **244**, 738.
- Black, J. H.:1991, in T. W. Hartquist (ed.), *Molecular Astrophysics*, Cambridge University Press, Cambridge, U.K., p. 473.
- Blanchard, A., Valls-Gabaud, D., and Mamon, G. A.:1992, *Astron. Astrophys.*, **264**, 365.
- Blondin, J. M.:2000, *New Astron.*, **5**, 53.
- Blumenthal, G. R., Faber, S. M., Primack, J. R., and Rees, M. J.: 1984, *Nature*, **311**, 517.
- Bodenheimer, P.:1995, *Ann. Rev. Astron. Astrophys.*, **33**, 505.
- Bodenheimer, P. and Sweigart, A.:1968, *Astrophys. J.*, **152**, 515.
- Bond, J. R., Cole, S., Efstathiou, G., and Kaiser, N.:1991, *Astrophys. J.*, **379**, 440.
- Bonnor, W. B.:1957, *Monthly Not. Roy. Astron. Soc.*, **117**, 104.
- Braun, E. and Dekel, A.:1989, *Astrophys. J.*, **345**, 31.
- Bromm, V. and Larson, R. B., 2004, *Ann. Rev. Astron. Astrophys.*, **42**, 79.
- Bromm, V. and Loeb, A.:2003, *Astrophys. J.*, **596**, 34.
- Bromm, V. and Loeb, A.:2004, *New Astron.*, **9**, 353.

- Bromm, V., Coppi, P. S., and Larson, R. B.:1999, *Astrophys. J.*, **527**, L5.
- Bromm, V., Coppi, P. S., and Larson, R. B.:2002, *Astrophys. J.*, **564**, 23.
- Bromm, V., Yoshida, N., and Hernquist, L.:2003, *Astrophys. J.*, **596**, L135.
- Bryan, G. L. and Norman, M. L.:1997a, in D. A. Clarke and M. Fall (eds.), *Computational Astrophysics (ASP Conference Series 123)*, Astronomical Society of the Pacific, p. 363.
- Bryan, G. L. and Norman, M. L.:1997b, in N. Chrisochoides (ed.), *Workshop on Structured Adaptive Mesh Refinement Grid Methods*, Springer-Verlag, p. 165.
- Bryan, G. L. and Norman, M. L.:1998, *Astrophys. J.*, **495**, 80.
- Carlberg, R. G.:1981, *Monthly Not. Roy. Astron. Soc.*, **197**, 1021.
- Carroll, S. M., Press, W. H., and Turner, E. L.:1992, *Ann. Rev. Astron. Astrophys.*, **30**, 499.
- Ciardi, B. and Ferrara, A., 2004, *Space Science Rev.*, in press.
- Cojazzi, P., Bressan, A., Lucchin, F., Pantano, O., and Chavez, M.:2000, *Monthly Not. Roy. Astron. Soc.*, **315**, L51.
- Cooray, A. and Sheth, R.:2002, *Phys. Rep.*, **372**, 1.
- Couchman, H. M. P., Thomas, P. A., and Pearce, F. R.:1995, *Astrophys. J.*, **452**, 797.
- Dalgarno, A. and Lepp, S.:1987, in M. S. Vardya and S. P. Tarafdar (eds.), *Astrochemistry (IAU Symp. 120)*, D. Reidel Publishing Co., Dordrecht, p. 109.
- de Araujo, J. C. N. and Opher, R.:1989, *Monthly Not. Roy. Astron. Soc.*, **239**, 371.
- Doroshkevich, A. G. and Kolesnik, I. G.:1976, *Sov. Astron.*, **20**, 4.
- Eggleton, P. P., Faulkner, J., and Flannery, B. P.:1973, *Astron. Astrophys.*, **23**, 325.
- Elmegreen, B. G.:1993, *Astrophys. J.*, **419**, L29.
- Elmegreen, B. G. and Scalo, J.:2004, *Ann. Rev. Astron. Astrophys.*, submitted; astro-ph/0404451.
- Fan, X., Narayanan, V. K., Lupton, R. H., Strauss, M. A., Knapp, G. R., Becker, R. H., White, R. L., Pentericci, L., Leggett, S. K., Haiman, Z., Gunn, J. E., Ivezić, Z., Schneider, D. P., *et al.*:2001, *Astron. J.*, **122**, 2833.
- Fan, X., Strauss, M. A., Schneider, D. P., Becker, R. H., White, R. L., Haiman, Z., Gregg, M., Pentericci, L., Grebel, E. K., Narayanan, V. K., *et al.*:2003, *Astron. J.*, **125**, 1649.
- Field, G. B.:1965, *Astrophys. J.*, **142**, 531.
- Fleck, R. C., Jr.:1982, *Monthly Not. Roy. Astron. Soc.*, **201**, 551.
- Flower, D. R.:2002, *Monthly Not. Roy. Astron. Soc.*, **333**, 763.
- Flower, D. R. and Pineau des Forêts, G.:2001, *MNRAS*, **323**, 672.
- Flower, D. R. and Pineau des Forêts, G.:2003, *Monthly Not. Roy. Astron. Soc.*, **341**, 1272.
- Foster, P. N. and Chevalier, R. A.:1993, *Astrophys. J.*, **416**, 303.
- Frank, J., King, A., and Raine, D.:1995, *Accretion Power in Astrophysics (2nd ed.)*, Cambridge University Press, U.K.
- Freedman, W. L., Madore, B. F., Gibson, B. K., Ferrarese, L., Kelson, D. D., Sakai, S., Mould, J. R., Kennicutt, R. C., Jr., *et al.*:2001, *Astrophys. J.*, **553**, 47.
- Fryer, C. L., Woosley, S. E., and Heger, A.:2001, *Astrophys. J.*, **550**, 372.
- Fuller, T. M. and Couchman, H. M. P.:2000, *Astrophys. J.*, **544**, 6.
- Galli, D. and Palla, F.:1998, *Astron. Astrophys.*, **335**, 403.
- Gammie, C. F.:2001, *Astrophys. J.*, **553**, 174.
- Gammie, C. F., Lin, Y. T., Stone, J. M., and Ostriker, E. C.:2003, *Astrophys. J.*, **592**, 203.
- Gingold, R. A. and Monaghan, J. J.:1977, *Monthly Not. Roy. Astron. Soc.*, **181**, 375.

- Glover, S. C. O.:2001, PhD thesis, Edinburgh University.
- Glover, S. C. O.:2003, *Astrophys. J.*, **584**, 331.
- Glover, S. C. O. and Brand, P. W. J. L.:2001, *Monthly Not. Roy. Astron. Soc.*, **321**, 385.
- Gnedin, N. Y.:1995, *Astrophys. J. Suppl.*, **97**, 231.
- Gnedin, N. Y.:1996a, *Astrophys. J.*, **456**, 1.
- Gnedin, N. Y.:1996b, *Astrophys. J.*, **456**, 34.
- Gnedin, N. Y. and Abel, T.:2001, *New Astron.*, **6**, 437.
- Gnedin, N. Y. and Bertschinger, E.:1996, *Astrophys. J.*, **470**, 115.
- Gnedin, N. Y. and Hui, L.:1998, *Monthly Not. Roy. Astron. Soc.*, **296**, 44.
- Gnedin, N. Y. and Ostriker, J. P.:1997, *Astrophys. J.*, **486**, 581.
- Goldreich, P. and Lynden-Bell, D.:1965, *Monthly Not. Roy. Astron. Soc.*, **130**, 97.
- Gott, J. R. and Thuan, T. X.:1976, *Astrophys. J.*, **204**, 649.
- Gould, R. J. and Salpeter, E. E.:1963, *Astrophys. J.*, **138**, 393.
- Gray, M. E., Taylor, A. N., Meisenheimer, K., Dye, S., Wolf, C., and Thommes, E.:2002, *Astrophys. J.*, **568**, 141.
- Haehnelt, M. G.:1995, *Monthly Not. Roy. Astron. Soc.*, **273**, 249.
- Haiman, Z. and Loeb, A.:1997, *Astrophys. J.*, **483**, 21.
- Haiman, Z., Thoul, A., and Loeb, A.:1996, *Astrophys. J.*, **464**, 523.
- Hasegawa, T., Yoshii, Y., and Sabano, Y.:1981, *Astron. Astrophys.*, **98**, 186.
- Hayes, J. C. and Norman, M. L.:2003, *Astrophys. J. Suppl.*, **147**, 197.
- Heger, A., Fryer, C. L., Woosley, S. E., Langer, N., and Hartmann, D. H.:2003, *Astrophys. J.*, **591**, 288.
- Heitsch, F., Mac Low, M.-M., and Klessen, R. S.:2001, *Astrophys. J.*, **547**, 280.
- Hernquist, L. and Katz, N.:1989, *Astrophys. J. Suppl.*, **70**, 419.
- Hofmann, S., Schwarz, D. J., and Stöcker, H.:2001, *Phys. Rev. D*, **64**, 083507.
- Hollenbach, D. and McKee, C. F.:1979, *Astrophys. J. Suppl.*, **41**, 555.
- Hoyle, F.:1953, *Astrophys. J.*, **118**, 513.
- Hummer, D. G. and Rybicki, G. B.:1971, *Monthly Not. Roy. Astron. Soc.*, **152**, 1.
- Hunter, C.:1962, *Astrophys. J.*, **136**, 594.
- Hunter, C.:1964, *Astrophys. J.*, **139**, 570.
- Hunter, C.:1977, *Astrophys. J.*, **218**, 834.
- Hutchins, J. B.:1976, *Astrophys. J.*, **205**, 103.
- Iglesias, C. A. and Rogers, F. J.:1996, *Astrophys. J.*, **464**, 943.
- Jang-Condell, H. and Hernquist, L.:2001, *Astrophys. J.*, **548**, 68.
- J Jeans, J. H.:1902, *Phil. Trans. A*, **199**, 1.
- J Jeans, J. H.:1928, *Astronomy and Cosmogony*, Cambridge University Press, U.K.
- Jenkins, A., Frenk, C. S., White, S. D. M., Colberg, J. M., Cole, S., Evrard, A. E., Couchman, H. M. P., and Yoshida, N.:2001, *Monthly Not. Roy. Astron. Soc.*, **321**, 372.
- Johnson, B. M. and Gammie, C. F.:2003, *Astrophys. J.*, **597**, 131.
- Kirkman, D., Tytler, D., Suzuki, N., O'Meara, J., and Lubin, D.:2003, *Astrophys. J. Suppl.*, **149**, 1.
- Kitsionas, S. and Whitworth, A. P.:2002, *Monthly Not. Roy. Astron. Soc.*, **330**, 129.
- Klessen, R. S., Heitsch, F., and Mac Low, M.-M.:2000, *Astrophys. J.*, **535**, 887.
- Kogut, A., Spergel, D. N., Barnes, C., Bennett, C. L., Halpern, M., Hinshaw, G., Jarosik, N., Limon, M., Meyer, S. S., and Page, L.:2003, *Astrophys. J. Suppl.*, **148**, 161.
- Kudritzki, R. P.:2002, *Astrophys. J.*, 2002, **577**, 389.
- Kulsrud, R. M., Cen, R., Ostriker, J. P., and Ryu, D.:1997, *Astrophys. J.*, **480**, 481.
- Lacey, C. G.:1989, *Astrophys. J.*, **336**, 612.

- Lahav, O.:1986, *Monthly Not. Roy. Astron. Soc.*, **220**, 259.
- Larson, R. B.:1969, *Monthly Not. Roy. Astron. Soc.*, **145**, 271.
- Larson, R. B.:1973, *Fund. Cosm. Phys.*, **1**, 1.
- Larson, R. B.:1981, *Monthly Not. Roy. Astron. Soc.*, **194**, 809.
- Larson, R. B.:1984, *Monthly Not. Roy. Astron. Soc.*, **206**, 197.
- Larson, R. B.:1985, *Monthly Not. Roy. Astron. Soc.*, **214**, 379.
- Larson, R. B.:1990, *Monthly Not. Roy. Astron. Soc.*, **243**, 588.
- Larson, R. B.:2002, *Monthly Not. Roy. Astron. Soc.*, **332**, 155.
- Larson, R. B. and Starrfield, S.:1971, *Astron. Astrophys.*, **13**, 190.
- Latter, W. B. and Black, J. H.:1991, *Astrophys. J.*, **372**, 161.
- Layzer, D.:1963, *Astrophys. J.*, **137**, 351.
- Le Bourlot, J., Pineau des Forêts, G., and Flower, D.:1999, *Monthly Not. Roy. Astron. Soc.*, **305**, 802.
- Lenzuni, P., Chernoff, D. F., and Salpeter, E. E.:1991, *Astrophys. J. Suppl.*, **76**, 759.
- Lepp, S. and Shull, J. M.:1983, *Astrophys. J.*, **270**, 578.
- Lepp, S. and Shull, J. M.:1984, *Astrophys. J.*, **280**, 465.
- Lepp, S., Buch, V., and Dalgarno, A.:1995, *Astrophys. J. Suppl.*, **98**, 345.
- Li, Y., Klessen, R. P., and Mac Low, M.-M.:2003, *Astrophys. J.*, **592**, 975.
- Li, P. S., Norman, M. L., Mac Low, M.-M., and Heitsch, F.:2004, *Astrophys. J.*, **605**, 800.
- Lin, C. C., Mestel, L., and Shu, F. H.:1965, *Astrophys. J.*, **142**, 1431.
- Lin, D. N. C. and Murray, S. D.:1992, *Astrophys. J.*, **394**, 523.
- Lin, D. N. C. and Murray, S. D.:2000, *Astrophys. J.*, **540**, 170.
- Lin, D. N. C. and Papaloizou, J. C. B.:1993, in E. H. Levy and J. I. Lunine (eds.), *Protostars and Planets III*, University of Arizona Press, Tucson, U.S.A., p. 749.
- Lin, D. N. C. and Pringle, J. E.:1987, *Monthly Not. Roy. Astron. Soc.*, **225**, 607.
- Low, C. and Lynden-Bell, D.:1976, *Monthly Not. Roy. Astron. Soc.*, **176**, 367.
- Lucy, L. B.:1977, *Astron. J.*, **82**, 1013.
- Mac Low, M.-M.:1999, *Astrophys. J.*, **524**, 169.
- Mac Low, M.-M. and Klessen, R. P.:2004, *Rev. Mod. Phys.*, **76**, 125.
- Mac Low, M.-M. and Shull, J. M.:1986, *Astrophys. J.*, **302**, 585.
- Maret, S., Ceccarelli, C., Caux, E., Tielens, A. G. G. M., and Castets, A.:2002, *Astron. Astrophys.*, **395**, 573.
- Marigo, P., Chiosi, C., and Kudritzki, R.-P.:2003, *Astron. Astrophys.*, **399**, 617.
- Masunaga, H. and Inutsuka, S.:1999, *Astrophys. J.*, **510**, 822.
- Mather, J. C., Cheng, E. S., Eplee, R. E., Jr., Isaacman, R. B., Meyer, S. S., Shafer, R. A., Weiss, R., Wright, E. L., Bennett, C. L., Boggess, N. W., *et al.*:1990, *Astrophys. J.*, **354**, L37.
- Matsuda, T., Sato, H., and Takeda, H., *Prog. Theor. Phys.*, **42**, 219.
- Matzner, C. D. and McKee, C. F.:1999, *Astrophys. J.*, **526**, L109.
- McDowell, M. R. C.:1961, *Observatory*, **81**, 240.
- McKee, C. F. and Zweibel, E. G.:1992, *Astrophys. J.*, **399**, 551.
- McNally, D. and Settle, J. J.:1980, *Monthly Not. Roy. Astron. Soc.*, **192**, 917.
- Meiksin, A., White, M., and Peacock, J. A.:1999, *Monthly Not. Roy. Astron. Soc.*, **304**, 851.
- Miyama, S. M., Hayashi, C., and Narita, S.:1984, *Astrophys. J.*, **279**, 621.
- Miyama, S. M., Narita, S., and Hayashi, C.:1987a, *Prog. Theor. Phys.*, **78**, 1051.
- Miyama, S. M., Narita, S., and Hayashi, C.:1987b, *Prog. Theor. Phys.*, **78**, 1273.
- Mo, H. J. and White, S. D. M.:2002, *Monthly Not. Roy. Astron. Soc.*, **336**, 112.
- Monaghan, J. J.:1992, *Ann. Rev. Astron. Astrophys.*, **30**, 543.

- Moore, B., Ghigna, S., Governato, F., Lake, G., Quinn, T., Stadel, J., and Tozzi, P.:1999, *Astrophys. J.*, **524**, L19.
- Murray, S. D. and Lin, D. N. C.:1990, *Astrophys. J.*, **363**, 50.
- Murray, S. D. and Lin, D. N. C.:1996, *Astrophys. J.*, **467**, 728.
- Myers, P. C.:2000, *Astrophys. J.*, **530**, L119.
- Nakamura, F. and Umemura, M.:1999, *Astrophys. J.*, **515**, 239.
- Nakamura, F. and Umemura, M.:2001, *Astrophys. J.*, **548**, 19.
- Nakamura, F. and Umemura, M.:2002, *Astrophys. J.*, **569**, 549.
- Nakano, T., Hasegawa, T., and Norman, C.:1995, *Astrophys. J.*, **450**, 183.
- Nakano, T., Hasegawa, T., Morino, J.-I., and Yamashita, T.:2000, *Astrophys. J.*, **534**, 976.
- Navarro, J. F. and Steinmetz, M.:2000, *Astrophys. J.*, **528**, 607.
- Nishi, R. and Susa, H.:1999, *Astrophys. J.*, **523**, L103.
- Nomura, H. and Mineshige, S.:2000, *Astrophys. J.*, **536**, 429.
- Norman, M. L.:2003, private communication.
- Norman, M. L.:2004, in Plewa, T., Linde, T., and Weirs, V. G. (eds.), *Adaptive Mesh Refinement – Theory and Applications*, Springer-Verlag, in press; astro-ph/0402230.
- Norman, M. L., Wilson, J. R., and Barton, R. T.:1980, *Astrophys. J.*, **239**, 968.
- Oh, S. P. and Haiman, Z.:2002, *Astrophys. J.*, **569**, 558.
- Oliveira, S. R., Miranda, O. D., de Araujo, J. C. N., and Opher, R.:1998a, *Monthly Not. Roy. Astron. Soc.*, **301**, 101.
- Oliveira, S. R., Miranda, O. D., de Araujo, J. C. N., and Opher, R.:1998b, *Monthly Not. Roy. Astron. Soc.*, **301**, 115.
- O’Meara, J. M., Tytler, D., Kirkman, D., Suzuki, N., Prochaska, J. X., Lubin, D., and Wolfe, A. M.:2001, *Astrophys. J.*, **552**, 718.
- Omukai, K.:2000, *Astrophys. J.*, **534**, 809.
- Omukai, K.:2001, *Astrophys. J.*, **546**, 635.
- Omukai, K. and Inutsuka, S.:2002, *Monthly Not. Roy. Astron. Soc.*, **332**, 59.
- Omukai, K. and Nishi, R.:1998, *Astrophys. J.*, **508**, 141.
- Omukai, K. and Nishi, R.:1999, *Astrophys. J.*, **518**, 64.
- Omukai, K. and Palla, F.:2001, *Astrophys. J.*, **561**, L55.
- Omukai, K. and Palla, F.:2003, *Astrophys. J.*, **589**, 677.
- Omukai, K. and Yoshii, Y.:2003, *Astrophys. J.*, **599**, 746.
- Ostriker, E. C., Gammie, C. F., and Stone, J. M.:1999, *Astrophys. J.*, **513**, 259.
- Ostriker, J.:1964, *Astrophys. J.*, **140**, 1056.
- Ostriker, J. P. and Gnedin, N. Y.:1996, *Astrophys. J.*, **472**, L63.
- Padoan, P.:1995, *Monthly Not. Roy. Astron. Soc.*, **277**, 377.
- Padoan, P. and Nordlund, Å.:2002, *Astrophys. J.*, **576**, 870.
- Padoan, P., Nordlund, Å., and Jones, B. J. T.:1997, *Monthly Not. Roy. Astron. Soc.*, **288**, 145.
- Palla, F., Salpeter, E. E., and Stahler, S. W.:1983, *Astrophys. J.*, **271**, 632.
- Parker, E. N.:1953, *Astrophys. J.*, **117**, 431.
- Passot, T. and Vázquez-Semadeni, E.:1998, *Phys. Rev. E*, **58**, 4501.
- Peebles, P. J. E.:1980, *The Large Scale Structure of the Universe*, Princeton University Press, Princeton, N.J., U.S.A.
- Peebles, P. J. E. and Dicke, R. H.:1968, *Astrophys. J.*, **154**, 891.
- Pen, U.-L.:1998, *Astrophys. J. Suppl.*, **115**, 19.
- Penston, M. V.:1969, *Monthly Not. Roy. Astron. Soc.*, **144**, 425.

- Percival, W. J., Baugh, C. M., Bland-Hawthorn, J., Bridges, T., Cannon, R., Cole, S., Colless, M., Collins, C., Couch, W., Dalton, G., *et al.*:2001, *Monthly Not. Roy. Astron. Soc.*, **327**, 1297.
- Perlmutter, S., Aldering, G., Goldhaber, G., Knop, R. A., Nugent, P., Castro, P. G., Deustua, S., Fabbro, S., Goobar, A., Groom, D. E., *et al.*: 1999, *Astrophys. J.*, **517**, 565.
- Pöppel, W. G. L.:1975, *Astrophys. Space Sci.*, **32**, 175.
- Press, W. H. and Schechter, P.: 1974, *Astrophys. J.*, **187**, 425.
- Rawlings, J. M. C., Drew, J. E., and Barlow, M. J.:1993, *Monthly Not. Roy. Astron. Soc.*, **265**, 968.
- Rees, M.:1976, *Monthly Not. Roy. Astron. Soc.*, **176**, 483.
- Rees, M. J. and Ostriker, J. P.:1977, *Monthly Not. Roy. Astron. Soc.*, **179**, 541.
- Ricotti, M., Gnedin, N. Y., and Shull, J. M.:2002a, *Astrophys. J.*, **575**, 33.
- Ricotti, M., Gnedin, N. Y., and Shull, J. M.:2002b, *Astrophys. J.*, **575**, 47.
- Riess, A. G., Filippenko, A. V., *et al.*:1998, *Astron. J.*, **116**, 1009.
- Ripamonti, E. and Abel, T.:2004, *Monthly Not. Roy. Astron. Soc.*, **348**, 1019.
- Ripamonti, E., Haardt, F., Ferrara, A., and Colpi, M.:2002, *Monthly Not. Roy. Astron. Soc.*, **334**, 401.
- Sabano, Y. and Yoshii, Y.:1977, *Pub. Astron. Soc. Japan*, **29**, 207.
- Saslaw, W. C. and Zipoy, D.:1967, *Nature*, **216**, 976.
- Saumon, D., Chabrier, G., and van Horn, H. M.:1995, *Astrophys. J. Suppl.*, **99**, 713.
- Savedoff, M. P. and Vila, S.:1962, *Astrophys. J.*, **136**, 609.
- Scalo, J. and Elmegreen, B. G.:2004, *Ann. Rev. Astron. Astrophys.*, submitted; astro-ph/0404452.
- Seljak, U.:2000, *Monthly Not. Roy. Astron. Soc.*, **318**, 203.
- Seljak, U. and Zaldarriaga, M.:1996, *Astrophys. J.*, **469**, 437.
- Shakura, N. I. and Sunyaev, R. A.:1973, *Astron. Astrophys.*, **24**, 337.
- Shapiro, P. R. and Kang, H.:1987, *Astrophys. J.*, **318**, 32.
- Sheth, R. K. and Tormen, G.:1999, *Monthly Not. Roy. Astron. Soc.*, **308**, 119.
- Shu, F. H.:1977, *Astrophys. J.*, **214**, 488.
- Stahler, S. W., Shu, F. H., and Taam, R. E.:1980a, *Astrophys. J.*, **241**, 637.
- Stahler, S. W., Shu, F. H., and Taam, R. E.:1980b, *Astrophys. J.*, **242**, 226.
- Stahler, S. W., Shu, F. H., and Taam, R. E.:1981, *Astrophys. J.*, **248**, 727.
- Stodólkiewicz, J. S.:1963, *Acta Astronomica*, **13**, 30.
- Silk, J.:1977a, *Astrophys. J.*, **211**, 638.
- Silk, J.:1977b, *Astrophys. J.*, **214**, 152.
- Silk, J.:1982, *Astrophys. J.*, **256**, 514.
- Silk, J.:1983, *Monthly Not. Roy. Astron. Soc.*, **205**, 705.
- Silk, J. and Suto, Y.:1988, *Astrophys. J.*, **335**, 295.
- Singh, S. and Ma, C.-P.:2002, *Astrophys. J.*, **569**, 1.
- Smoot, G. F. Bennett, C. L., Kogut, A., Wright, E. L., *et al.*:1992, *Astrophys. J.*, **396**, L1.
- Spergel, D. N., Verde, L., Peiris, H. V., Komatsu, E., Nolta, M. R., Bennett, C. L., Halpern, M., Hinshaw, G., Jarosik, N., Kogut, A., *et al.*:2003, *Astrophys. J. Suppl.*, 2003, **148**, 175.
- Springel, V., Yoshida, N., and White, S. D. M.:2001, *New Astron.*, **6**, 79.
- Spruit, H. C.:1987, *Astron. Astrophys.*, **184**, 173.
- Stachniewicz, S. and Kutschera, M.:2003, *Monthly Not. Roy. Astron. Soc.*, **339**, 616.
- Stahler, S. W., Palla, F., and Salpeter, E. E.:1986a, *Astrophys. J.*, **302**, 590.
- Stahler, S. W., Palla, F., and Salpeter, E. E.:1986b, *Astrophys. J.*, **308**, 697.
- Stancil, P. C., Lepp, S., and Dalgarno, A.:1998, *Astrophys. J.*, **509**, 1.

- Stancil, P. C., Lepp, S. H., and Dalgarno, A.:2002, *J. Phys. B*, **35**, 57.
- Stone, J. M., Ostriker, E. C., and Gammie, C. F.:1998, *Astrophys. J.*, **508**, L99.
- Suginohara, T. and Suto, Y.:1991, *Pub. Astron. Soc. Pacific*, **43**, L17.
- Susa, H., Uehara, H., and Nishi, R.:1996, *Prog. Theor. Phys.*, **96**, 1073.
- Susa, H., Uehara, H., Nishi, R., and Yamada, M.:1998, *Prog. Theor. Phys.*, **100**, 63.
- Tan, J. C. and Blackman, E. G.:2004, *Astrophys. J.*, **603**, 401.
- Tan, J. C. and McKee, C. F.:2003, in S. Holt and C. Reynolds (eds.), *The Emergence of Cosmic Structure (AIP Conf. Proc. 666)*, American Institute of Physics, p. 93.
- Tan, J. C. and McKee, C. F.:2004, *Astrophys. J.*, **603**, 383.
- Tegmark, M., Silk, J., Rees, M., Blanchard, A., Abel, T., and Palla, F.:1997, *Astrophys. J.*, **474**, 1.
- Thoul, A. A. and Weinberg, D. H.:1995, *Astrophys. J.*, **442**, 480.
- Tohline, J. E.:1980, *Astrophys. J.*, **239**, 417.
- Tohline, J. E.:1981, *Astrophys. J.*, **248**, 717.
- Tohline, J. E.:1982, *Fund. Cosm. Phys.*, **8**, 1.
- Toomre, A.:1964, *Astrophys. J.*, **139** 1217.
- Truelove, J. K., Klein, R. I., McKee, C. F., Holliman, J. H., Howell, L. H., and Greenough, J. A.:1997, *Astrophys. J.*, **489**, L179.
- Tsuribe, T. and Inutsuka, S.:1999a, *Astrophys. J.*, **523**, L155.
- Tsuribe, T. and Inutsuka, S.:1999b, *Astrophys. J.*, **526**, 307.
- Tsuribe, T. and Inutsuka, S.:2001, *Astrophys. and Space Sci.*, **276**, 1097.
- Uehara, H. and Inutsuka, S.:2000, *Astrophys. J.*, **531**, L91.
- Uehara, H., Susa, H., Nishi, R., Yamada, M., and Nakamura, T.:1996, *Astrophys. J.*, **473**, L95.
- Valentine, H., Saunders, W., and Taylor, A.:2000, *Monthly Not. Roy. Astron. Soc.*, **319**, L13.
- Villere, K. R. and Bodenheimer, P. H., 1987, in M. S. Vardya and S. P. Tarafdar (eds.), *Astrochemistry (IAU Symp. 120)*, D. Reidel Publishing Co., Dordrecht, p. 121.
- Ward-Thompson, D., André, P., and Kirk, J. M.:2002, *Monthly Not. Roy. Astron. Soc.*, **329**, 257.
- Whalen, D., Abel, T., and Norman, M. L.:2003, *Astrophys. J.*, submitted; astro-ph/0310283.
- Whitworth, A. P.:1998, *Monthly Not. Roy. Astron. Soc.*, **296**, 442.
- Whitworth, A. P. and Summers, D.:1985, *Monthly Not. Roy. Astron. Soc.*, **214**, 1.
- Widrow, L. M.:2002, *Rev. Mod. Phys.*, **74**, 775.
- Wolfire, M. G. and Cassinelli, J. P.:1987, *Astrophys. J.*, **319**, 850.
- Yoneyama, T.:1972, *Pub. Astron. Soc. Japan*, **24**, 87.
- Yoshida, N., Bromm, V., and Hernquist, L.:2004, *Astrophys. J.*, **605**, 579.
- Yoshida, N., Abel, T., Hernquist, L. and Sugiyama, N.:2003, *Astrophys. J.*, **592**, 645.
- Yoshida, N., Sokasian, A., Hernquist, L., and Springel, V.:2003, *Astrophys. J.*, **591**, L1.
- Yoshii, Y. and Sabano, Y.:1979, *Pub. Astron. Soc. Japan*, **31**, 505.
- Yoshii, Y. and Sabano, Y.:1980, *Pub. Astron. Soc. Japan*, **32**, 229.
- Zeldovich, Y. B.:1970, *Astron. Astrophys.*, **5**, 84.

